
10

MUSCLE FORCE AND MYOELECTRIC MANIFESTATIONS OF MUSCLE FATIGUE IN VOLUNTARY AND ELECTRICALLY ELICITED CONTRACTIONS

R. MERLETTI,¹ B. AFSHARIPOUR,¹ J. DIDERIKSEN,² AND D. FARINA²

¹*Laboratory for Engineering of the Neuromuscular System, Politecnico di Torino, Torino, Italy*

²*Department of Neurorehabilitation Engineering, Universitätsmedizin Göttingen, Georg-August-Universität, Göttingen, Germany*

10.1 INTRODUCTION

Muscles produce force under voluntary control or under control of an external drive (e.g., electrical stimulation). Muscles also produce a distribution of electrical potential over the skin (sEMG). During sustained voluntary or electrically stimulated contractions, as well as during intermittent or dynamic contractions, both force and sEMG undergo changes that are referred to as mechanical and myoelectric manifestations of muscle fatigue.

The study of these mechanical and electrical phenomena has many applications in sport (to improve and quantify performance), in rehabilitation medicine (to monitor recovery), in occupational medicine (to prevent and monitor work-related disorders), and in many other fields such as space medicine, prostheses control, and oncology.

While force, torque or EMG voltage are well-defined physical quantities, this is not the case with muscle fatigue.

Many definitions of muscle fatigue exist. Mechanical manifestations of muscle fatigue are defined as an exercise-induced reduction in the maximal force generating capacity of a muscle and may be attributed to (a) changes of muscle drive by the central nervous system (central fatigue) and (b) changes of muscle force generating capability (peripheral fatigue) [56,57]. Myoelectric manifestations of muscle fatigue are defined as changes of features of the sEMG during sustained muscle activity. These features reflect both central and peripheral phenomena leading to mechanical fatigue and are detectable much earlier than mechanical failure.

Since, at this time, the force applied by a muscle to its tendons cannot be measured directly, changes of sEMG have been used for over a century as indirect indicators of muscle force and fatigue [104]. The single-channel sEMG parameters and algorithms used for this purpose have been described in Chapter 4 and will be only briefly recalled in this chapter.

The use of sEMG to “guess” the contraction level (force) or the fatigue condition of a muscle can be extremely misleading. Competence in the physiology and biophysics of sEMG generation is required to avoid common traps and misinterpretations. Doctors in occupational, sport, and rehabilitation medicine, as well as other clinicians and therapists, dream of techniques or instruments that could quantify force and fatigue in dynamic conditions during daily life activities, work activities, sport training, or rehabilitation exercises. While most of this is becoming technically feasible, the interpretation of the information derived from the sEMG signals is still difficult (often impossible) because of the large number of phenomena and physical variables reflected by sEMG and of confounding factors [44]. While these factors are being unraveled, relatively simple test conditions can provide indications about the performance of a muscle (or a group of muscles) in specific settings such as isometric constant force contractions, isometric variable force contractions (typically ramps), and some simple dynamic tasks.

This chapter deals with the association between sEMG and force/fatigue and outlines this association, the tools to study it, the many limitations and drawbacks of the available techniques, and the open questions that remain to be solved.

10.2 JOINT TORQUE MEASUREMENT AND MUSCLE FORCE ESTIMATION IN ISOMETRIC CONTRACTIONS

10.2.1 Joint Torque Measurements in Isometric Contractions

Skeletal muscles act on rigid body segments—that is, on bones—that are assumed to be connected by a hinge and rotate around a pivot point (center of rotation). This is an approximation that allows us to define the lever arm of the muscle force and to establish the association between muscle force and torque applied to a joint such as the elbow or knee. Isometric braces lock two body segments, preventing their

relative movement, and load cells (with fixed lever arm) or torque meters measure the produced torque. A number of conditions arise concerning these measurements: (a) If torque meters are used, they must be aligned with the center of rotation of the joint, and (b) if a load cell is used, the lever arm of the measured force with respect to the center of rotation must be known to estimate torque. If measurements are performed at a fixed joint angle and only relative torque values (expressed as percentage of the maximum torque) are of interest, these conditions can be somewhat relaxed. The position of the brace and of the body segments may affect the results [37]. For example, the arm (or the thigh) can be either vertical or horizontal and the forearm (or the leg) can be at different angles. The weight of the forearm or leg should be compensated for by adjusting the offset of the measuring instrument in relaxed conditions. A force target is presented to the subject on a computer screen or other display and the subject is asked to match it (constant force isometric conditions) or track it (variable force isometric condition). The target is often a percentage of a previously measured maximal voluntary contraction (MVC). Lack of consensus exists on how MVC should be measured; the average or the peak value of 3–5 short (3–5 s) contractions are often used. This protocol is referred to as a force control task.

Another alternative, for the elbow or knee joints, is to have the subject hold a weight attached to the wrist (arm vertical and forearm horizontal) or to the ankle (trunk horizontal, thigh vertical, and leg horizontal) and hold the required position. This protocol is referred to as a position control task and usually no feedback is given. The neurophysiological control strategy is very different from that of the previous protocol. Among other things, the second protocol leads to a shorter endurance time. For details see the extensive work of Enoka et al. [31,32].

10.2.2 Surface EMG-Based Joint Torque Estimation in Isometric Contractions

Among the many purposes of the investigations described in the previous section one is to establish a relationship between sEMG and muscle force, and another one is to study the sEMG changes reflecting fatigue in isometric conditions with constant or variable torque (ramps or intermittent contractions).

These issues have been investigated for over six decades [65,121,122]; many of them are still open and unsolved, despite new approaches (see Chapter 9). One of these issues concerns the fact that the torque measured with an isometric brace is due to many muscles (agonists, antagonists, mono- or bi-articular). The only exception is the first dorsal interosseous (FDI) which is the only agonist muscle acting on the thumb-index joint: this is why it has been investigated so often [18,19,141,142]. As opposed to force, sEMG, in general, refers mostly to one muscle only. The sEMG amplitude and frequency features depend on the location, size, and interelectrode distance of the electrode pair (see Chapters 2 and 5). In addition, deeply located motor units contribute little to the sEMG features but contribute fully to the produced and measured force/torque. As an extreme

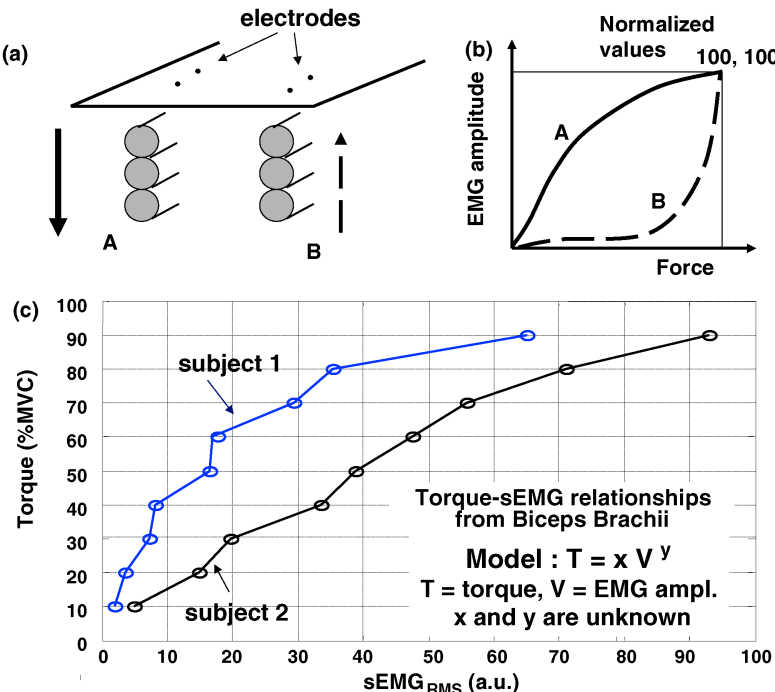


FIGURE 10.1 (a) Schematic extreme examples of two muscles with order of recruitment of the motor units from top-down and from bottom-up. (b) General pattern of the sEMG amplitude versus muscle force for the two cases depicted in part a. (c) Experimental plots of isometric elbow torques versus the average RMS value of the longitudinal single differential sEMG signals obtained from a grid (13 rows \times 5 columns, IED = 10 mm) placed, on the biceps brachii, proximally with respect to the innervation zone. The two curves are obtained from two healthy subjects. A possible mathematical model is indicated for the relationship torque = $f(sEMG_{RMS})$. The model implies that the torque is produced only by the biceps brachii.

example, a subject could co-contract agonists and antagonists, producing little or no net torque at the joint but high sEMG from either muscle group.

Figure 10.1a depicts two extreme examples of muscles recruiting motor units from the superficial ones to the deep ones (muscle A) or from the deep ones to the superficial ones (muscle B). Because of the effect of recruitment order (small motor units first) and of distance between the sources and the electrodes, as force increases, the sEMG increases, usually nonlinearly, with the concavity down (A) or up (B) as indicated qualitatively in Fig. 10.1b. These are *not* the only reasons determining the degree of nonlinearity; motor unit size and algebraic summation (cancellation) of motor unit action potentials (MUAP) are additional reasons [49].

Figure 10.1c depicts the relationship between isometric elbow torque and RMS of the sEMG in two healthy subjects. An electrode grid (13 rows and 5 columns with interelectrode distance of 10 mm) was placed on the biceps brachii (proximal with

respect to the innervation zone), and the RMSs of all the longitudinal single differential channels were averaged to get a representative sEMG RMS value over a 10-s epoch (see Chapter 5). Voluntary torque was increased in steps of 10% MVC and sustained for 10 s at each level.

Different curves are observed for the two subjects. The two plots of Fig. 10.1b, as well as any monotonously increasing pattern in between these extremes, could be approximated by the mathematical relation described in Eq. (10.1), where T is the torque contributed by the muscle, V is an sEMG amplitude indicator (e.g., RMS or ARV), and x and y are unknown real coefficients defining the curve.

$$T = xV^y \quad (\text{for } y > 0) \quad (10.1)$$

For $0 < y < 1$, concavity is down; for $y = 1$, the relationship is a straight line; for $y > 1$, concavity is up; the sign of x indicates agonist or antagonist muscle [1]. Obviously, T cannot be measured for a single muscle. In the case of the elbow flexion, we have the biceps (short and long head), the brachioradialis, and the brachialis muscles on the agonist side, and we have the three heads of the triceps brachii on the antagonist side. If we consider T as the total measured torque, Eq. (10.1) is not correct since the sEMG is obtained from only one muscle while T is produced by many muscles. To simplify the problem, one may assume that the antagonists are off and the agonists are all pulling at the same percentage of their MVC, but this is not necessarily true. A simple example involving only two muscles is given in Fig. 10.2 and a system of equations based on the mathematical model proposed above is given in Eqs. (10.2–10.5), describing two muscles and four contraction levels. T_i is the total (known) torque at contraction level i ($i = 1, 2, 3, 4$), $V_{i,j}$ is the (known) RMS (or other amplitude parameter) of muscle j at contraction level i , and x_1 , y_1 , x_2 , and y_2 are the unknown

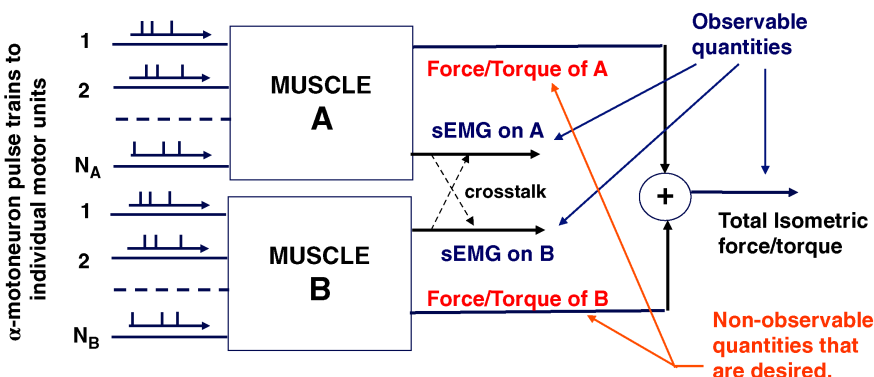


FIGURE 10.2 Input and output variables for two muscles (A and B) acting on the same joint. Inputs are the action potential trains of the N_A and N_B motor neurons. Outputs are the produced force and sEMG amplitude detected from a pair of electrodes or from an electrode grid. Crosstalk may be affecting the signals. Observable and nonobservable quantities are indicated.

model coefficients for muscle 1 and 2.

$$T_1 = x_1 V_{1,1}^{y_1} + x_2 V_{1,2}^{y_2} \quad (10.2)$$

$$T_2 = x_1 V_{2,1}^{y_1} + x_2 V_{2,2}^{y_2} \quad (10.3)$$

$$T_3 = x_1 V_{3,1}^{y_1} + x_2 V_{3,2}^{y_2} \quad (10.4)$$

$$T_4 = x_1 V_{4,1}^{y_1} + x_2 V_{4,2}^{y_2} \quad (10.5)$$

Equations (10.2)–(10.5) provide a system of four nonlinear equations (one for each contraction level), with four unknowns, whose solution(s) provide the unknown model coefficient x_i and y_i which define the torque contributed by each muscle. The x_1 and x_2 unknowns can be obtained from two of the equations and substituted in the other two obtaining a system of two equations and two unknowns (y_1 and y_2 appearing at the exponent) which can be solved either numerically, or by optimization methods by minimizing the mean square error between the measured and the model-predicted torques [right sides of Eqs. (10.2)–(10.5)] [1].

In the given example, the number of contractions and equations could be greater than four when an optimization method is used for finding the solution(s). It is interesting to observe that more than one solution may be obtained, suggesting that more than one load sharing strategy is compatible with the torque outputs. The algorithm can be generalized to more than two muscles (for M muscles at least $2M$ equations—that is, $2M$ contraction levels—are needed) and can be applied to subsequent epochs of a fatiguing contraction to observe the changes of the x_i and y_i coefficients and therefore estimate the initial load sharing among the muscles acting on a joint as well as its evolution in time. The algorithm is still under investigation and testing [1].

Figure 10.3 shows an example where the sEMG signals are measured from the two heads of the biceps (as one muscle), the brachioradialis, and two heads of the triceps using electrode grids and arrays and estimating the average envelope of the sEMG RMS over selected channels of each electrode system. The solution is obtained using an optimization algorithm (particle swarm optimization [105]). Because of difficulties in reading the sEMG of the deep muscles (brachialis and medial head of the triceps), the contributions of these muscles cannot be accounted for and are incorporated in those of the others, causing estimation errors. Periodic “parameter estimation”—that is, updating of the x_i and y_i parameters during a test such as that of Fig. 10.3—would provide information about the changes of the torque–sEMG relationship of the individual muscles during a fatiguing exercise.

The model described above is purely mathematical. Its validation is not easy since the contraction force of individual muscles cannot be measured. However, some indirect measurements based on ultrasound technology may become available in the near future [8] and provide means of validation. Other models of force or torque generation offer closer correlation with physiological quantities. Among these is the model proposed by Fuglevand et al. [54] and the more recent and comprehensive model proposed by Dideriksen et al. [23] and applied to the investigation of the

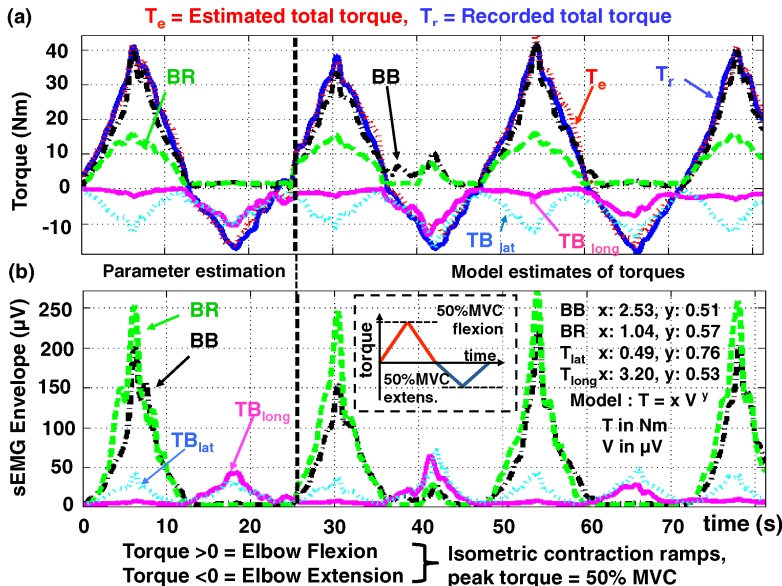


FIGURE 10.3 Example of application of the model described in Eqs. (10.2)–(10.5). The elbow of the subject was locked in an isometric brace and he was tracking a torque target on a computer screen producing a sequence of flexion–extension cycles ranging between 50% MVC flexion and 50% MVC extension (see inset in panel b). Single differential sEMG was detected, with four electrode arrays, from the biceps brachii (BB), the brachioradialis (BR), and the long and lateral heads of the triceps (TB_{long} , TB_{lat}) (signals from the brachialis and the medial head of the triceps could not be detected). The RMS envelopes were averaged over the channels showing activity. The Particle Swarm Optimization algorithm was used to find the x_i and y_i values that minimized the mean square error between the estimated total torques and the measured ones. The first cycle (25 s, parameter estimation) was used to estimate the x_i and y_i muscle parameters which were then used to estimate the total torque and the contributions of the individual muscles in the subsequent cycles (model estimates of torques). **(a)** Plots of the recorded and estimated torque and of the contributions of the individual muscles considered. Such contributions include those of the not considered muscles (brachialis and medial head of the triceps). **(b)** Plots of RMS envelopes of the considered muscles. The target profile is provided in the inset on the left. The x and y values of the model $T = xV^y$ are provided in the inset on the right for each muscle. It is interesting to notice the co-contraction of agonist and antagonist muscles, which is presumably implemented for better tracking of the force target. The anatomical definition of TB_{lat} and TB_{long} is according to Saladin, K. S., *Anatomy & Physiology: The Unity of Form and Function*, 3rd ed., McGraw-Hill, New York, 2003.

sEMG–force relation and of fatigue [24]. Dynamic musculoskeletal models are discussed in Chapter 9.

10.2.3 Reading sEMG for Force Estimation

The models described above imply the availability of representative sEMG amplitude values. Although these values can be obtained from pairs of electrodes placed over

individual muscles, 2D electrode arrays can provide spatial averages over a region of interest (ROI) defined as a portion of a sEMG map. Electrode grids provide maps of sEMG distribution from which a single indicator of sEMG amplitude (ARV or RMS) can be extracted for each observable muscle and introduced in a force estimation algorithm such as the one defined in Eqs. (10.2)–(10.5). This procedure implies segmentation of the map into ROIs from which the spatial average of ARV or RMS may be obtained, as explained below. Amplitude estimates of individual sEMG channels may be obtained with the algorithms described in Chapter 4.

Figure 10.4 outlines the distribution of single differential sEMG RMS over the arm and forearm of a healthy subject performing various tasks. In this protocol, three

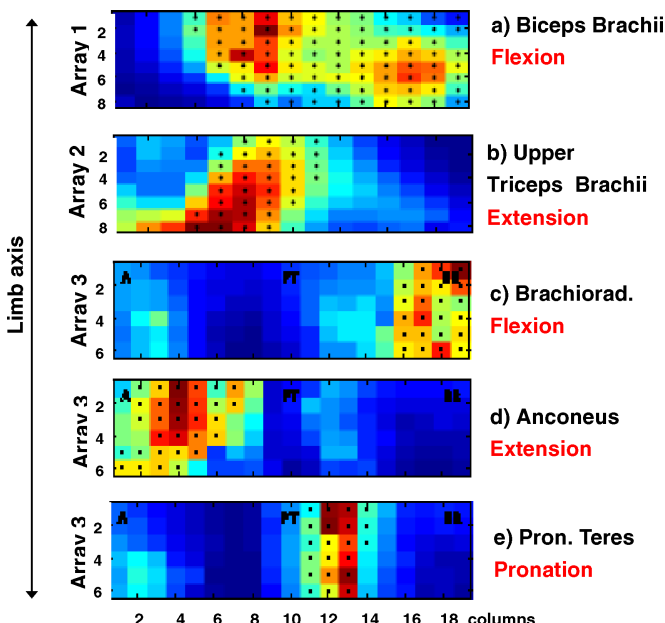


FIGURE 10.4 Examples of single differential sEMG maps obtained from three 2-D arrays, each made with silver-coated eyelets filled with conductive gel, spaced 10 mm apart (8 or 6 rows and 19 columns) and fixed on a cloth. The arrays were applied to the distal part of the biceps brachii (array 1), proximal part of triceps brachii (array 2), and proximal portion of the forearm (array 3), with the columns parallel to the longitudinal direction of the limb. Array 3 covered the anconeus, brachioradialis, and pronator teres muscles (A, PT, BR). Isometric elbow flexion, extension, and forearm pronation were performed at 50% of the MVC of each task. The features of sEMG (amplitude in this case) were estimated over a region of interest, where the signals corresponding to a specific effort are stronger and presumably due to a single muscle. These regions are defined by means of segmentation algorithms and are identified by black dots. Panel a shows the contributions of the two heads of the biceps. The average of the amplitudes, (ARV or RMS) of the pixels marked with a dot provides a sEMG value for that muscle—to be used, for example, in a model such as the one defined by Eqs. (10.2)–(10.5). The same applies to the other panels.

electrode arrays (8 or 6 rows \times 20 columns in the fiber direction, IED = 10 mm) were placed respectively across the biceps brachii (array 1), on the triceps brachii (array 2), and on the proximal portion of the forearm (array 3) with the columns aligned with the limb axis. The elbow joint was locked in an isometric brace; efforts of elbow flexion, extension, and forearm pronation were performed at about 50% MVC for 10 s, where MVC was previously measured for each task. The RMS values were computed on a 5-s epoch. Regions of interest (ROI) were identified with an image segmentation method and were indicated with a black dot on each pixel of the ROI [114].

10.3 PHYSIOLOGICAL MECHANISMS OF MUSCLE FATIGUE: A MODELING APPROACH

Different types and definitions of muscle fatigue exist and have been proposed and discussed in the literature. Some are based on the inability to sustain a required force/torque (mechanical manifestations of muscle fatigue), others are based on the force increment elicited by electrical stimulation during a fatiguing contraction (interpolated twitch) [62,84,119], and others are based on the changes that specific features of the sEMG undergo during sustained efforts or tasks [18,19,87,88]. These latter changes may or may not be related to mechanical modifications of performance, take place from the beginning of the contraction, and reflect the muscle drive and the phenomena taking place at the muscle fiber membrane level even in the absence of force changes; they are referred to as myoelectric manifestations of muscle fatigue [19,88,93].

Muscle force is centrally modulated by varying the number of active motor units and their discharge rates [14,20]. Muscle force is also determined by the proper functioning of the neuromuscular junctions, by the sarcolemma excitability, by the excitation–contraction coupling, and by the contractile mechanisms inside the fibers. Some of these mechanisms are affected by blood flow which is blocked at high contraction levels [16,120], causing the muscle to operate in ischemic conditions with progressive accumulation of metabolites [24,25].

All these mechanisms play a role in sustaining force and may fail at different times and in different degrees. These mechanisms have been addressed by De Luca [18,19] and discussed in the book *Fatigue: Neural and Muscular Mechanisms* [56] and in more recent reviews [32]. Although there are still considerable gaps of knowledge concerning the role of these mechanisms and their interactions, it is well known that sEMG features change, during a sustained contraction, without a concurrent change in muscle force and vice versa; therefore the sEMG–force relationship, described in Section 10.2.2, changes as fatigue develops.

Recent modeling efforts contributed to unravel these complex relations. To simulate the motor neuron discharge patterns in fatigue, the model of motor neuron pool behavior and isometric force developed by Fuglevand et al. [54] was adopted and extended by Dideriksen et al. [23–25]. These authors developed a model that accounts for the accumulation of metabolic substances within the muscle, the depletion of energy, and the occlusion of blood flow related to the sustained contraction. The

simulated concentration of metabolites determines the degree of inhibitory afferent feedback to the motor neuron pool [58] as well as the changes in the twitch force. The metabolites diffuse, across the cell membranes, into the extracellular space from which they are removed by the bloodstream.

A control algorithm has been implemented [23,24] to (a) simulate sustained contractions at a constant force level while the excitability of the motor neuron pool and its force producing capability change and (b) estimate the descending drive needed to maintain a stable force output. As fatigue progresses, this model adjusts the descending drive to compensate for the neuromuscular changes. At a certain point, the descending drive reaches its maximal level, making it impossible to maintain the target force (task failure).

The intramuscular action potential at different stages of muscle fatigue was described by Dimitrova and Dimitrov [26–28]. According to this description, as fatigue develops, the duration of the intracellular action potential increases and its amplitude decreases. In the Dideriksen model [23], these changes are associated with (i) the metabolite concentration, (ii) the conduction velocity of the muscle fibers of the motor unit, and (iii) the instantaneous discharge rate of the motor unit and its size. Having established the shape of the intracellular action potential, its appearance on the surface is simulated using the model of volume conduction in the muscle, fat, and skin tissue between the single muscle cell and the electrode [45] (see Chapters 2 and 8). In this way, a complete set of motor unit action potentials across different levels of force and fatigue can be generated, the interference sEMG can be simulated and its amplitude (RMS) can be calculated.

Figure 10.5 shows results from a simulated ramp contraction from zero to maximal force. The average motor unit conduction velocity spans the range from no fatigue (~ 5 m/s) to severe fatigue (~ 3 m/s). The sEMG amplitude corresponding to every combination of muscle activation level and motor unit conduction velocity is determined and represented in a three-dimensional plot.

Figure 10.5 also indicates that an increase in the muscle activity (number of motor unit discharges per second) always involves an increase in the sEMG amplitude. The gain of this relation, however, is slightly higher at low levels of muscle activation, suggesting that the same increase in the muscle activation implies a higher increase in the sEMG amplitudes at low activation levels compared to higher levels. This observation can be explained by a difference in the level of sEMG amplitude cancellation (due to the algebraic summation of MUAPs) of approximately 20% across the range of muscle activations.

As conduction velocity decreases from the nonfatigue values (4–5 m/s), the corresponding sEMG amplitude increases. A peak of sEMG amplitude is reached around conduction velocities of 3.2 m/s, after which the sEMG amplitude decreases because the decrease in amplitude predominates on the increase in the action potential duration [28]. It should be noted that not all the values in the figure are physiologically realistic since the muscle activation level and conduction velocity are not independent variables (for example, conditions yielding the supramaximal amplitudes ($\sim 130\%$) do not occur in normal conditions). In sustained submaximal contractions at constant force levels, the muscle activation level is expected to start at a submaximal level and

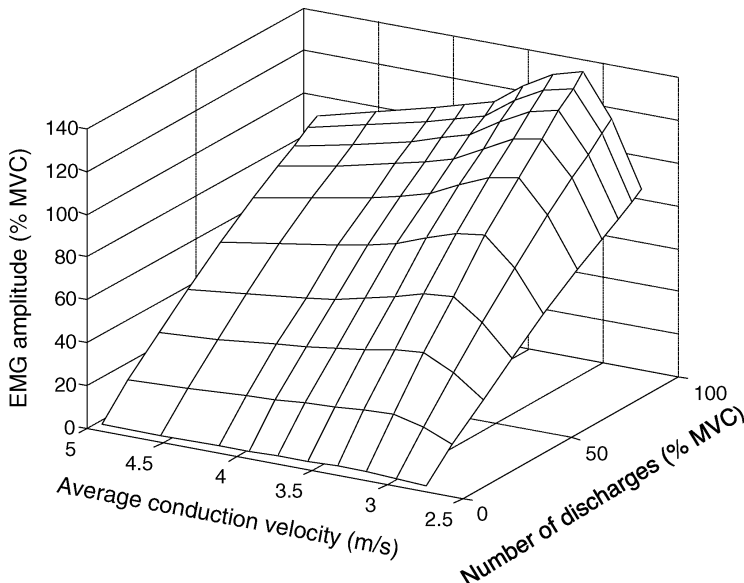


FIGURE 10.5 The simulated relation between EMG amplitude, average muscle fiber conduction velocity, and muscle activation (number of motor unit discharges per second for the entire motor unit population). Adapted from Dideriksen et al. [25].

increase slightly to compensate for the adaptations in motor neuron excitability and contractile properties whereas the conduction velocity decreases. In typical fatigue studies, however, minimal conduction velocities are rarely lower than 3.2 m/s [58] and thus are in the part of the curve where it causes the sEMG amplitude to increase. Therefore, the model predicts that sustained contractions would imply a modest contribution of conduction velocity to the increases in the sEMG amplitude, which is in accordance with experimental observations [81].

Although sEMG and muscle force are direct reflections of the activity of muscles (Figs. 10.1 and 10.2), differences in the adaptations of the action potentials and the force producing capacity may progressively modify their relationship. This was demonstrated in another series of simulations by Dideriksen et al. [24,25] which included a series of sustained contractions at constant force levels, trapezoidal contractions, and repeated ramp contractions. In Fig. 10.6 each thin line represents the time course of the concurrently simulated sEMG amplitude versus force across the different simulation paradigms. The lower dashed, curved line indicates the non-fatigue case, whereas the upper dashed line indicates the relation in severe fatigue. The figure demonstrates that a sEMG amplitude value of 60% of the maximal sEMG value may correspond to forces in the range from 10% to 50% MVC depending on the level of fatigue of the muscle. This very large range indicates that adaptations to fatigue can significantly modulate the sEMG–force relation and that this modulation depends on the characteristics of the task. Therefore, the experimental sEMG–force

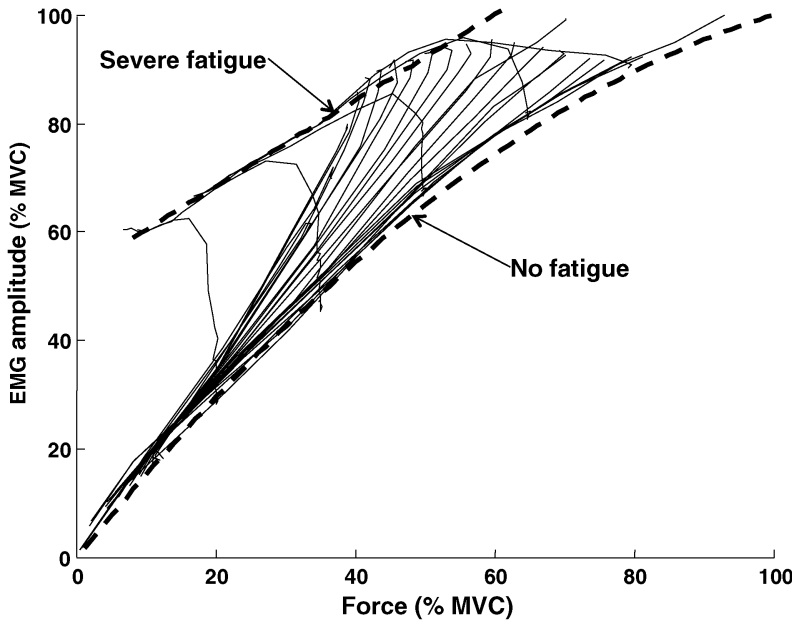


FIGURE 10.6 The simulated relation between EMG amplitude and force across multiple different simulation paradigms. The dashed lines indicate the boundaries for this relation at different levels of fatigue. Reprinted from Dideriksen et al. [24].

relationship indicated in Fig. 10.1c can be estimated only at the beginning of a moderately fatiguing contraction and the muscle parameters x_i and y_i in Eqs. (10.2–10.5) may be changing during a sustained contraction.

Motor unit mechanical twitches produce displacements of the skin above the muscle which can be detected with microphones or accelerometers. The resulting signal, referred to as mechanomyogram, is discussed in Chapter 11 of Merletti and Parker [92] and has been used as indicator of muscle fatigue [66,126].

The following sections of this chapter further deal with myoelectric manifestations of muscle fatigue and expand and update the material presented on this topic in Chapter 9 of Merletti and Parker [92] with specific focus of 2D sEMG.

10.4 MYOELECTRIC MANIFESTATIONS OF MUSCLE FATIGUE IN ISOMETRIC, CONSTANT FORCE, VOLUNTARY CONTRACTIONS

Myoelectric manifestations of muscle fatigue are defined as the changes taking place in the sEMG signal during a sustained muscle activity. As seen in the previous section, the relation between sEMG and muscle force is very complex and affected by many factors which also affect myoelectric manifestations of muscle fatigue. For this reason, myoelectric manifestations of muscle fatigue have been investigated in

conditions that eliminate some of these factors and allow the study of the remaining ones, reducing the likelihood of misinterpretation of results. Such conditions are obtained by implementing “bench-test” situations where the muscle(s) of interest operates under controlled conditions (for example, fixed length, fixed force, electrical activation, etc.). Since more than one agonist and more than one antagonist act on a joint (or on two joints), these conditions are difficult to achieve (see Section 10.2). For this reason the first dorsal interosseous (FDI) muscle has been extensively studied because it is the only agonist acting across the thumb–index joint [141,142]. In dynamic conditions, the shifting of the muscle under the skin substantially contributes to sEMG changes under an electrode pair, as explained in Section 10.5, often leading to signal misinterpretations. Further considerations on neurological mechanisms of muscle fatigue are provided in Chapter 12.

10.4.1 Quantification of Muscle Fatigue from sEMG in Isometric Constant Force Voluntary Contractions

The many factors affecting sEMG features, even during the simple experimental paradigm of sustained isometric constant-force contractions, range from anatomical features to the detection system to the estimation algorithm used [38–40,43,44]. The relevance of these factors depends on the produced force and on the joint angle. The two main factors are the decrease of muscle fiber conduction velocity (CV) (see Chapter 5) and the variations of shape and increase of the spatial support and time duration of the transmembrane action potential (intracellular action potential, IAP) [2,3,26,28]. The early work of Lindstrom, Chaffin, and De Luca [11,74,75,124] outlined how CV acts as a scaling factor for the sEMG and for its power spectrum, which is therefore compressed (shifted in logarithmic scale) by a decrease of CV (see Chapter 4).

In the ideal case where a general signal $x_1(\theta)$ is scaled in time (θ) to generate $x_2(\theta)=x_1(k\theta)$, its Fourier transform $X_2(f)$ and its power spectrum $P_2(f)=|X_2(f)|^2$ are scaled in frequency (and in amplitude) so that $X_2(f)=X_1(f/k)/k$ and $P_2(f)=P_1(f/k)/k^2$. This property applies to stochastic signals as well (see Fig. 4.1). Two characteristic frequencies have been used to describe sEMG spectral changes: the mean or centroid (MNF or f_{mean}) and the median (MDF or f_{med}). The latter is the 50th percentile of the power spectrum—that is, the value splitting it into two parts of equal area. Both frequencies are scaled by the same factor k . If the signal in time $x_1(\theta)$ is a sEMG generated by a source (e.g., a motor unit action potential) propagating in space with conduction velocity $CV(t)$ which is slowly decreasing with time (see Chapter 5), then, at time t , $CV(t)$ is a fraction of $CV(0)$, that is, $CV(t)=k CV(0)$. The coefficient k ($k < 1$) could be considered an indicator of myoelectric fatigue at time t . As a consequence, $f_{\text{mean}}(t)=kf_{\text{mean}}(0)$ and $f_{\text{med}}(t)=kf_{\text{med}}(0)$. If the decrement of CV were the **only** change taking place, the percent decrease of $f_{\text{mean}}(t)$ and $f_{\text{med}}(t)$ would be identical to the percent decrease of $CV(t)$ and their plots, normalized with respect to the respective initial values $CV(0)$, $f_{\text{mean}}(0)$, and $f_{\text{med}}(0)$, would overlap. In this case, k could be computed from the f_{mean} or the f_{med} of the power spectrum using a single-channel sEMG signal and could be used as an indicator of fatigue.

It can be shown that the inverse relation holds for the average rectified value of the signal (ARV) and for the root mean square (RMS, which is the square root of the area under the power spectrum). Specifically, $\text{ARV}(t) = \text{ARV}(0)/k$ and $\text{RMS}(t) = \text{RMS}(0)/\sqrt{k}$, indicating an increase of ARV and RMS associated to a decrease of CV. This increase is due to the widening and, therefore, to the increase of the area or the square of the absolute value, of the propagating motor unit action potentials. The plots of normalized CV, f_{mean} , f_{med} , ARV, and RMS (that is, the plots of k , $1/k$, and $1/\sqrt{k}$) are jointly and globally referred to as the “fatigue plot” [92].

A better way to obtain k is to use *all* spectral frequencies, rather than only f_{mean} or f_{med} . This method is referred to as the “cumulative power function method” and was originally proposed by H. Rix and Malengé [112] and applied to sEMG spectra by Merletti and Lo Conte [90]. The method provides the scaling factor between two frequency-scaled power spectra with similar but not identical shapes and outlines the regions where the shapes differ, as discussed in Chapter 4 and presented in Fig. 4.5.

Other factors, such as change of shape of the muscle and thickness of the subcutaneous tissue, also play a role [95]. In addition, the situation is different at different contraction levels. At a low contraction level, only a fraction of the muscle motor units are recruited (mostly small, type I), and dropout and replacement of motor units is possible. At medium levels of contraction, blood flow is almost occluded [119,120] and most motor units are recruited. At high levels of contraction, blood flow is fully occluded, all motor units are recruited, and motor unit substitution is no longer possible.

As indicated above, it should be noted that the rate of decrease of CV is not always matching that of MNF and MDF because:

1. Different motor units have different rates of change of CV. CV values have a statistical distribution that may change in time.
2. The active motor unit pool may change in time because of motor unit dropout and recruitment, and the synchronization of motor unit firings affects spectral variables.
3. The shape and width of the IAP may change.
4. The muscle fibers may not be parallel to the skin (pennate muscles) and CV cannot be measured.
5. The force produced by the muscle of interest may change, even if the total measured torque at the joint remains constant (different sharing of the load among the active muscles, see Section 10.2).
6. The degree of cancellation due to algebraic MUAP summation may change.

An example of sEMG detected with a linear electrode array during a low-level isometric torque (15% MVC sustained for 10 minutes) produced by a biceps brachii is provided in Fig. 10.7 [59]. The array has 8 electrodes, spaced 10 mm apart, and spans most of the muscle, and the signals are longitudinal single differential (LSD, along the fiber direction), thereby clearly showing the innervation zone in the middle of the

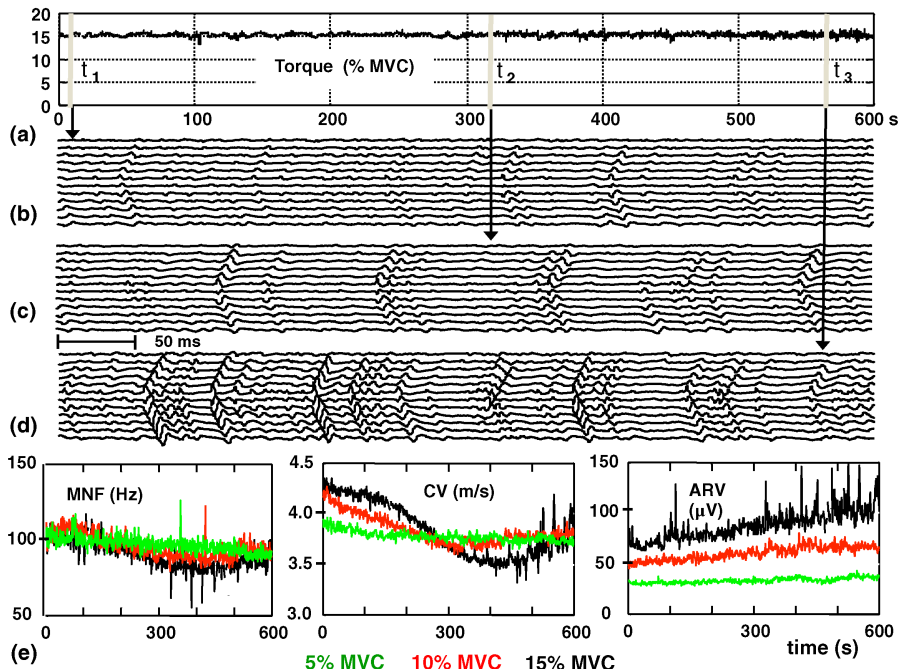


FIGURE 10.7 Isometric contraction of the biceps brachii of a healthy subject, sustained at 15% MVC for 10 minutes. (a) Torque plot. (b-d) sEMG signals detected with a linear electrode array (IED = 10 mm), centered on the muscle, during three 0.5-s epochs: one at the beginning, one in the middle, and one at the end of the contraction. (e) Plots of mean spectral frequency (MNF), muscle fiber conduction velocity (CV), and average rectified value during three 10-min contractions sustained at 5% MVC (green), 10% MVC (red), and 15% MVC (black). Observe the increase of MNF and CV, after 5 min, in the second and third case due to the recruitment of fresh motor units. Reprinted from Gazzoni et al. [59].

muscle. Three signal epochs of 0.5 s are depicted in panels b, c, and d (beginning of contraction, mid-contraction, end of contraction).

Even if there is no change in force (as indicated in panel a), the signals show the progressive recruitment of new motor units, suggesting that those recruited at the beginning are progressively less able to produce the required force. In this situation the definition of myoelectric manifestations of muscle fatigue becomes very questionable and the only meaningful definition is the one concerning the fatigue of individual motor units, which may be investigated after decomposition of the signals into the constituent motor unit action potential trains (Chapter 7). Mean spectral frequency values (MNF or f_{mean}) and the average rectified value (ARV) are computed for channels on either side of the innervation zone and averaged, and conduction velocity is computed using a group of channels on one side of the innervation zone (see Chapter 5). Figure 10.7e shows the time course of MNF, CV, and ARV corresponding

to three contraction levels (5% MVC, 10% MVC, 15% MVC). While the patterns of MNF and CV show a small decrement for the contraction level of 5% MVC, they show a decrement followed by an increment for 10% MVC and 15% MVC, reflecting fatigue of the initial motor unit pool followed by recruitment of fresh motor units.

The case described in Fig. 10.7 shows how carefully the changes of sEMG signals should be interpreted. For example, selecting a group of channels that include the innervation zone would provide erroneous results since CV cannot be defined, MNF and MDF have abnormally high values, and RMS and ARV have abnormally low values [44].

As discussed in Chapter 5, sEMG features can be defined in two dimensions, as maps above the skin. Figure 10.8 provides three maps of RMS and three maps of

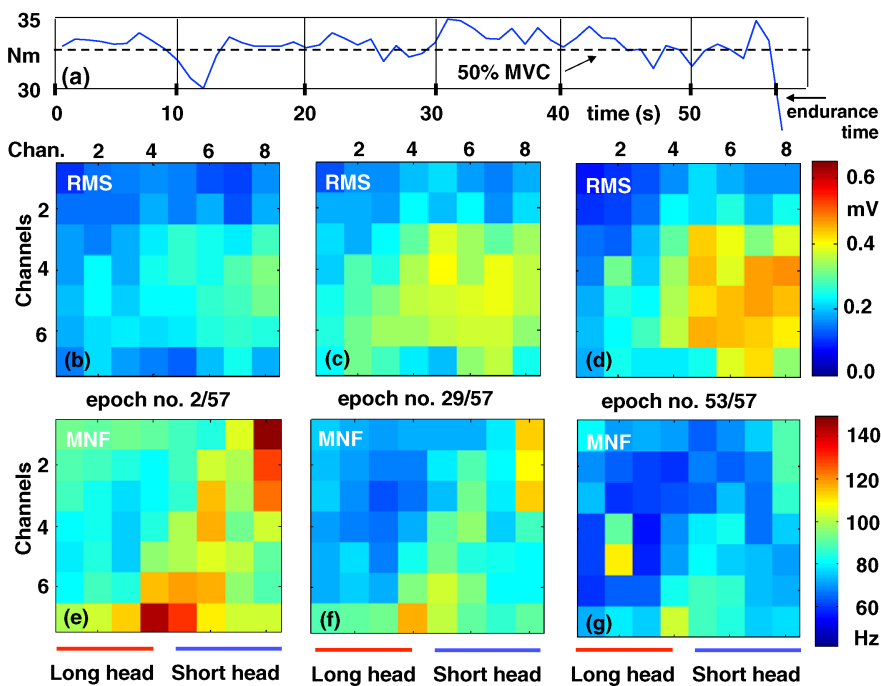


FIGURE 10.8 Isometric contraction of the left elbow flexors of a healthy subject, sustained at 50% MVC to endurance time (57 s). An electrode grid of 8×8 electrode (IED = 10 mm) is placed just proximal with respect to the innervation zone of the biceps brachii and sEMG detection is single differential along the columns, in the fiber direction. RMS and MNF are estimated on 57 one-second epochs. The left half of the grid is on the long head and the right part of the grid is on the short head of the muscle. No interpolation is applied. (a) Torque plot. (b-d) three maps of the RMS spatial distribution at epochs 2, 29 and 53; (e-g) three maps of the MNF spatial distribution at epochs 2, 29, and 53. The short head shows a marked increase of RMS values and a marked decrease of MNF values. The long head shows smaller initial values of the two variables and slightly smaller variations with time. No information is available about the torque contributed by these two muscles, and by other muscles acting on the elbow, to the total torque.

MNF obtained from a left biceps brachii using an electrode grid of 8×8 electrodes with IED = 10 mm (no interpolation). An isometric, constant flexion torque is produced at the elbow at 50% MVC and sustained to the endurance time (57 s) as indicated in Fig. 10.8a. For each longitudinal single differential signal the RMS and MNF values are computed over 1-s-long epochs and displayed as colors of the pixels. The columns of the grid are parallel to the fiber direction and the innervation zone of the muscle is just below the bottom row. The RMS and MNF maps are relative to epoch 2, 29, and 53. Panels b, c, and d show a progressive increase of RMS, particularly in the region of the short head. Panels e, f, and g show higher initial values of MNF and greater MNF decrease in the region of the short head. This figure demonstrates the possibility of studying localized myoelectric manifestations of muscle fatigue in individual muscle compartments.

Figure 10.9 shows maps of ARV and MNF estimated over 0.5-s epochs of single differential sEMG signals detected on the upper trapezius muscle during an isometric

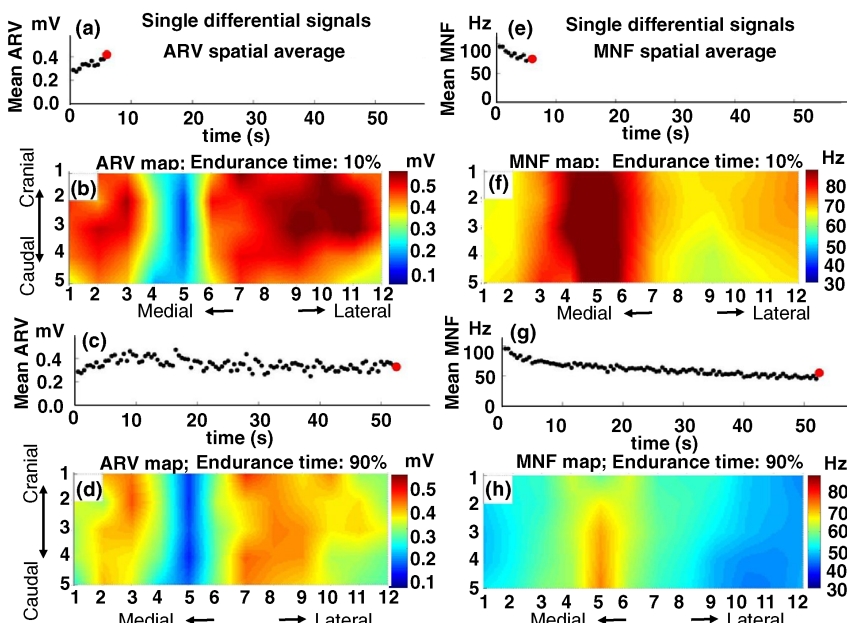


FIGURE 10.9 Fatigue study on the upper trapezius muscle of a healthy subject. The subject is pulling up a handle fixed to a load cell, with the straight vertical right arm, at 50% MVC. The effort is sustained to endurance (55 s). Single differential signals in the fiber direction are obtained using a 13×5 grid with IED = 8 mm. ARV and MNF are computed every 0.5 s and their maps are interpolated with a factor 10. (a) spatial average of ARV over the entire map every 0.5 s. (b) ARV map at the sixth second. (c) Spatial average of the ARV map at the 52nd second, few seconds before failure. (d) ARV map at the 52nd second. (e-h) Same plots and maps for MNF. Observe an important muscle innervation zone between rows 4 and 6 showing a valley in the ARV distribution and a peak in the MNF distribution.

contraction at 50% MVC sustained until endurance (55 s). The maps are obtained from a 13×5 grid with IED = 8 mm and are interpolated with a factor 10. The spatial averages of ARV and MNF, computed over a 1-s epoch and over the entire grid, are depicted in panels a and c for the 6th second of contraction and in panels e and g for the 52nd second of contraction, just before force failure. The valley of ARV and the peak of MNF on the innervation zone are evident. The initial increase of the spatially averaged ARV, followed by a decrease, and the progressive decrease of the spatially averaged MNF are also evident. No compartments or particular changes of image patterns can be clearly identified in this case. Similar results have been reported for monopolar and bipolar sEMG detection by other investigators [70,121,122] using smaller surface electrode arrays. The maps in Figs. 10.8 and 10.9 also show the importance of a topographic recording and point out how different bipolar sEMG signal could be when detected in different locations.

Other experiments demonstrated that topological changes of EMG distribution of the trapezius muscle take place during an isometric sustained contraction and that the entropy of the RMS image (degree of uniformity) decreases while the centroid of the image moves cranially [48]. These authors demonstrated that the subjects with more heterogeneous activity and larger shift of the image centroid towards the cranial direction could sustain the required isometric contraction force longer than subjects with more uniform activity and smaller centroid shift.

Other indices of fatigue have been investigated searching for those most sensitive, most repeatable or most focusing on specific central or peripheral mechanisms. Some examples are provided by Dimitrov et al. [26] who used spectral moments, other than the first, and their ratio as indicated in Eq. (10.6):

$$FI_k = \frac{\int_{f_1}^{f_2} f^{-1} P(f) df}{\int_{f_1}^{f_2} f^k P(f) df} \quad \text{for } k = 2, 3, 4, 5 \quad (10.6)$$

where $P(f)$ is the normalized power spectrum of the signal (spectrum with unit area), and f_1 and f_2 define the bandwidth over which the fatigue index FI is calculated. The integral at the denominator in Eq. (10.6) defines the moment of order k and the numerator is the moment of order -1 . The moment of order zero is the power of the signal—that is, its RMS².

Other authors proposed indices based on the fractal dimension (FD) [61,139] of the sEMG signal and the percentage of determinism (%DET, obtained from recurrence quantification analysis) [42,51,53]. Mesin et al. [94] compared the variability and the sensitivity of a number of fatigue indicators, applied to simulated stationary and nonstationary interferential signals, with respect to CV and motor unit synchronization changes. The coefficient of variation (COV) for stationary signals, computed over 60 epochs of 0.5 s each, turned out to be less than 0.5% for the estimated conduction velocity (ECV), between 1.5% and 4% for RMS, ARV, MNF, and MDF, between 4.5% and 9% for the FI indexes defined in Eq. (10.6), about 1% for entropy (S),

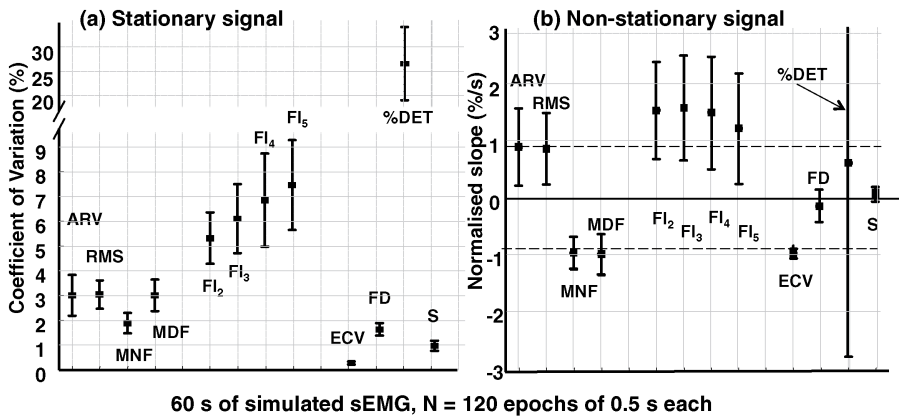


FIGURE 10.10 (a) Mean \pm st. dev. of the coefficient of variation (σ/mean in %) of a number of fatigue indicators calculated over 60 epochs of 0.5 s each of a simulated stationary EMG signal with no synchronization among motor units. An array of eight electrodes was simulated and the spatial mean of each feature was computed for each epoch. (b) Mean \pm st. dev. of the normalized slope (% of the initial value per second) of the same fatigue indicators calculated from nonstationary signals simulating a decrease of CV from 4 m/s to 3 m/s (0.83% of the initial value per second, indicated by the dashed lines) and an increase of synchronization from 9% to 20% in 30 s. The muscle fibers are parallel to the skin, and the array is on one side of the innervation zone. ARV and RMS: average rectified value and root mean square, MNF and MDF: mean and median frequency of the power spectrum, F₂, F₃, F₄, and F₅, are defined in Eq. (10.6). ECV, estimated muscle fiber conduction velocity; FD, fractal dimension; S, signal entropy; %DET, percentage of determinism obtained from the recurrence quantification analysis [42,53]. See text and Mesin et al. [94] for further details. Modified from [94] with permission.

between 1.5% and 2% for FD, and greater than 20% for %DET. Results from Mesin et al. [94] are indicated in Fig. 10.10a. The nonstationary signals were simulated (for fibers parallel to the skin) by imposing a distribution of motor unit CV values whose mean decreased linearly from 4 m/s to 3 m/s in 30 s (0.83% of the initial value per second) while synchronization (see definition in Mesin et al. [94]) increased linearly from 0% to 20% in 30 s. Results reported in Fig. 10.10b show (a) a nearly correct value of the mean slope of spectral variables (negative slope) and of amplitude variables (positive slope), (b) a higher sensitivity, associated with a greater variability, of the FI indexes defined in Eq. (10.6), (c) an estimate of CV (ECV) with small variability and slight bias, (d) small sensitivity of FD, and (e) a very large variability of %DET (see Mesin et al. [94] for details). The sensitivity of the estimated CV (ECV) is high with respect to variations of CV and low with respect to variations of motor unit synchronization, while the sensitivity of FD is low with respect to variations of CV and high with respect to variations of synchronization. These authors, therefore, proposed to define a fatigue index as a vector with two components, ECV and FD. The separate quantification of myoelectric manifestations of central and peripheral fatigue in clinical settings deserves further research.

The results reported above are relative to skin-parallel-fibered muscles and cannot be extrapolated to in-depth-pinnate muscle where most of the signal is due the end-of-fiber effect. In the in-depth-pinnate muscles spectral variables decrease with fatigue because of the progressive widening in time of the end-of-fiber effect consequent to the decreasing values of muscle fiber CV (which cannot be measured directly).

If an in-depth-pinnate muscle sustains an isometric constant force contraction, changes of spectral parameters may appear locally and correspond to the fiber-aponeurosis terminations of the active motor units. Gallina et al. [55] observed these localized myoelectric manifestations of muscle fatigue in the medial gastrocnemius muscle during a sequence of 5 s ON and 5 s OFF voluntary isometric contractions. Results are reported in Fig. 10.11.

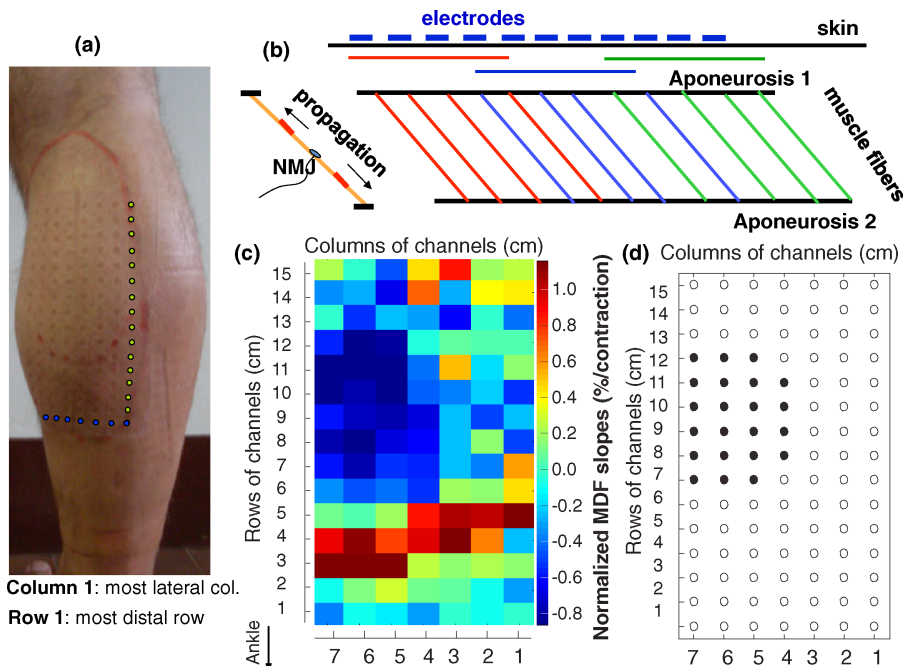


FIGURE 10.11 Localized myoelectric manifestations of fatigue in a pinnate muscle (medial gastrocnemius) observed by means of an electrode grid (16×7 electrodes, IED = 10 mm) during isometric intermittent contractions (5 s ON and 5 s Off). (a) Medial gastrocnemius region after removal of the grid, showing the locations of the electrodes. (b) Schematic arrangement of the fibers in the medial gastrocnemius. Three motor units are depicted, as an example, with fibers represented in red, blue, and green. Their signals would appear mostly in the red, blue, and green regions indicated under the electrodes. (c) Color map of the fatigue index “rate of decrement of MNF” defined as the slope (% of initial value per contraction) of the linear regression of MNF versus time for each electrode pair (longitudinal differential detection). (d) Segmented portion of the image showing high negative slope of MNF (see also Chapter 5).

The analysis of myoelectric manifestations of muscle fatigue in pinnate muscles requires considerable competence and understanding of the muscle structure and is an open field of research.

10.5 MYOELECTRIC MANIFESTATIONS OF MUSCLE FATIGUE IN DYNAMIC CONTRACTIONS

In dynamic conditions, the shifting of the muscle under the skin substantially contributes to sEMG changes under an electrode pair, as indicated in Fig. 10.12. These changes should *not* be interpreted as myoelectric manifestations of muscle fatigue. They are due to the change of muscle position under the skin, as demonstrated by the shift of the innervation zone (IZ). For this and other reasons, most studies have been carried out in isometric conditions or by reading the sEMG obtained at a fixed joint angle during cyclic

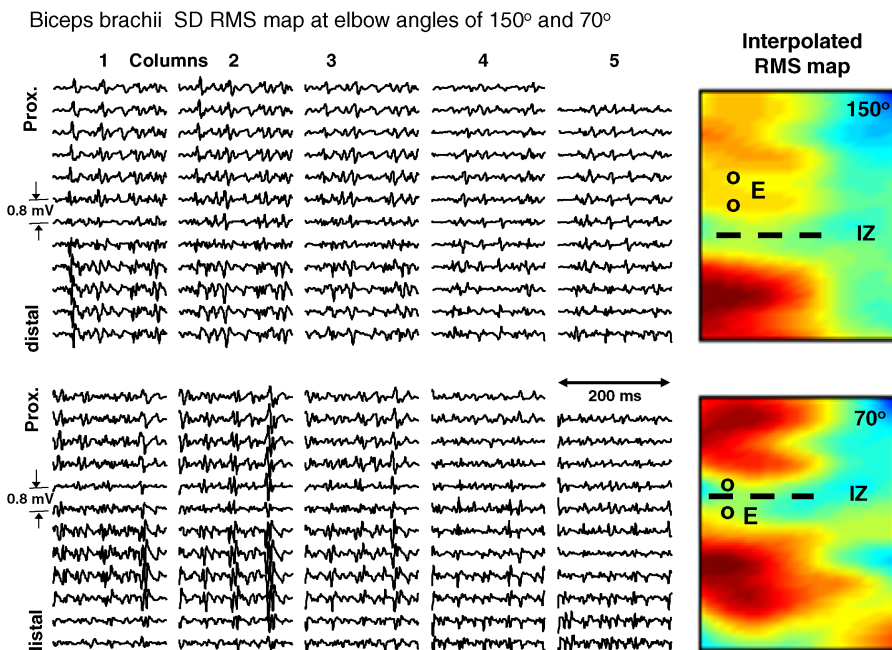


FIGURE 10.12 Effect of elbow angle on biceps EMG signals while the subject is holding a 3-kg weight in his hand and flexing the forearm with respect to the arm. Surface EMG signals were acquired in longitudinal single differential (LSD) mode from a biceps brachii muscle using a grid of 13 rows and 5 columns (columns along the limb direction, grid IED = 8 mm) at two elbow angles (150° and 70°). The image of RMS values is interpolated by a factor 10. As the elbow flexes from 150° to 70° the biceps shortens under the electrode grid and the innervation zone (thick dashed line) moves proximally by about 16 mm. The signals detected by the same pair of electrodes E in the two conditions are different because of the anatomical and geometrical changes rather than because of changes of muscle activation or force.

movements [5,6,99]. The muscle movement with respect to the skin and the electrodes is an important cause of signal change, in particular when a single electrode pair is used and the innervation zone moves under it (or away from it) during the movement. In the case of muscles with fibers parallel to the skin, an electrode array or a grid provides means to track the shift of the innervation zone and to read signals at a fixed distance from it [95].

The main problems arising in the study of fatigue in dynamic contractions are related to (a) the nonstationarity of the signal and (b) the relative movement of the muscle with respect to the electrodes. In the special case of cyclic movements (e.g., pedaling) short EMG epochs can be selected for feature extraction at the same fraction of each cycle.

In general, the study of nonstationary signals is addressed using the “time frequency representations” (TFR) which can be imagined as a short time spectrum evolving in time (time along the x axis, frequency along the y axis, and power represented by false colors) and providing a description of the time evolution of the “instantaneous” spectrum of the signal. Short bursts and explosive contractions can be analysed either with this method [5,6,68,99,119] or by the estimation of CV of individual multichannel MUAPs recorded during short sEMG bursts [106].

The Fourier expansion of a signal in series of basis functions (sinusoids) of infinite time support is appropriate for stationary signals with wide time support (high-frequency resolution and low-time resolution). A series expansion using basis functions with short time support is better suited to describe waves of short duration (motor unit action potential, M-waves) or signals that change rapidly in time (bursts). A family of expansions is based on a single shape (mother wavelet) from which the basis functions are obtained as scaled and shifted versions of the mother wavelet. Another family of expansions is based on non identical waveforms derived from the product of Gaussian functions and sinusoids (Gabor “wavelets”) or from the product of Gaussian functions and Hermite polynomials (Hermite “wavelets”) [79]. Applications to sEMG signals have been and are still being investigated [12,15,17,67,68].

10.6 MYOELECTRIC MANIFESTATIONS OF FATIGUE IN ELECTRICALLY ELICITED CONTRACTIONS

Mechanical and myoelectric manifestations of muscle fatigue are very relevant in functional electrical stimulation when electrically elicited contractions should be functionally efficient for a relatively long time. This section, however, deals mostly with myoelectric manifestations of muscle fatigue as investigation tools. Further discussions are presented in Chapter 11.

When a train of electric pulses is applied to a muscle motor point or to a motor nerve, the activated motor units discharge synchronously, producing a deterministic quasi-stationary signal, referred to as M-wave or compound motor action potential (CMAP), described in Fig. 4.4, as well as a twitch force. The number of recruited motor units depends on the amplitude and duration of the pulse according to the intensity-duration curve of the nerve fibers or of their terminal branches, as well as on

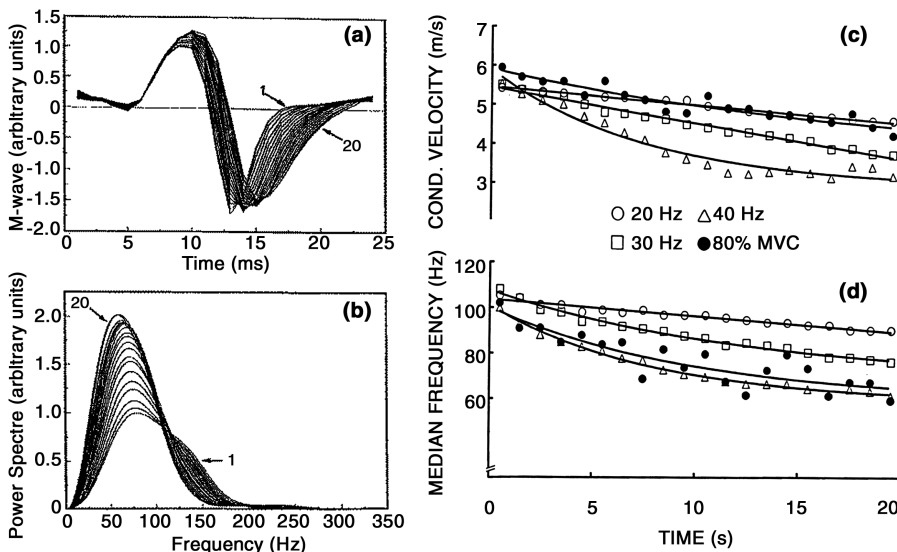


FIGURE 10.13 (a, b) Time evolution of a single differential M-wave elicited in the tibialis anterior (TA) muscle by motor point stimulation at 30 Hz* for 20 s (0.2-ms pulse duration). Each of the 20 waves is the average of 30 responses (1 s) and the power spectra are obtained by zero-padding to 1 s of each average M-wave. (c, d) Time course of conduction velocity (CV) and median frequency (MDF) during 20 s of stimulation of the TA at 20 Hz, 30 Hz, and 40 Hz. Black dots show the patterns detected in the same conditions during a voluntary contraction of the TA at 80% MVC. Note the widening of the M-wave and the compression of the spectrum, with increase of its area. Note the values of CV during the voluntary contraction being similar to those corresponding to 20 Hz stimulation, while the values of MDF decrease more, being sensitive to other factors such as the change of shape of the sources. Reproduced from [85] with permission.
 *: The currently used unit for stimulation frequency is “Hz” but “pulses/s” would be more appropriate.

geometrical factors (distance between such fibers and the electrodes) determining the current density at the nerve fiber level. Pulses are usually produced by current generators, rather than by voltage generators, to reduce the effect of changing electrode-skin impedance. Afferent fibers are activated as well; and the effect of their stimulation, which is relevant at low amplitudes and long pulse durations, is under investigation (see Chapters 11 and 12).

Figures 10.13a and 10.13b show the widening of the M-wave, along with the associated compression of the power spectral density, during an electrically elicited contraction of the tibialis anterior muscle (TA) sustained for 20 s at 30 Hz. Figures 10.13c and 10.13d show the decreasing pattern of conduction velocity (CV) and spectral median frequency (MDF) during 20 s of stimulation of the TA at 20 Hz, 30 Hz, and 40 Hz. For comparison, the same investigation included a voluntary contraction at 80% MVC, performed in the same conditions, whose results are shown as black dots in Figs. 10.13c and 10.13d [85,89].

It seems reasonable to think that each pulse of a train would produce a “quantum” of fatigue and therefore the fatigue-related changes of sEMG variables should be plotted

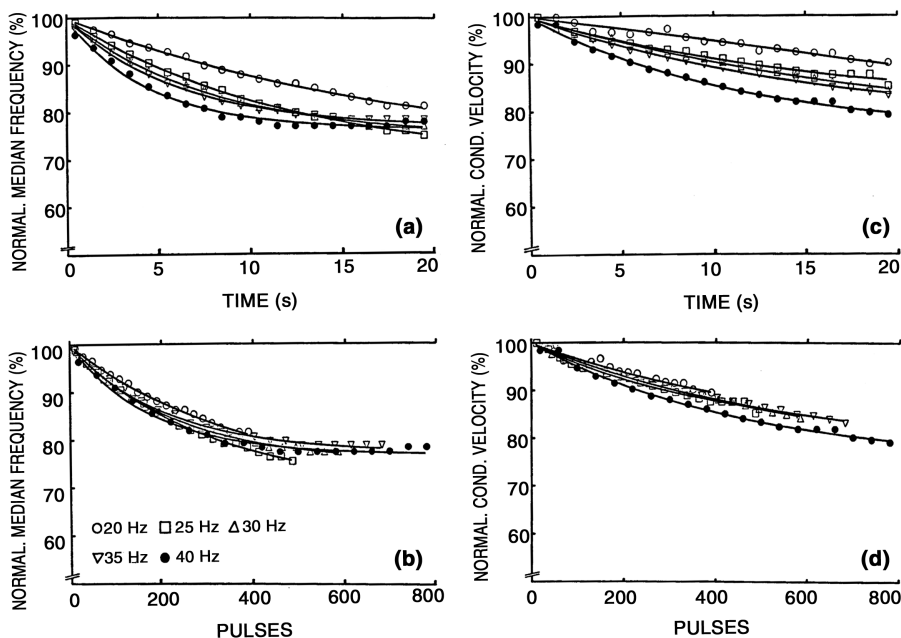


FIGURE 10.14 (a) Median frequency (normalized with respect to its initial value) of the power spectrum of the single differential sEMG detected on the tibialis anterior (TA) muscle during 20 s of electrical stimulation at 20 Hz, 25 Hz, 30 Hz, 35 Hz, and 40 Hz. (b) Same plot where the time scale has been replaced by the number of delivered pulses. (c) Normalized plot of conduction velocity (CV) in the same conditions as a). (d) Same plot as in part c, where the time scale has been replaced by the number of delivered pulses. The contractions are performed in isometric conditions and ankle torque shows a slight increase during each 20-s stimulation train due to widening of the mechanical twitch response (not shown in the figure). Reproduced from [89] with permission.

versus the number of delivered pulses rather than versus time, resulting in the same plot regardless of stimulation frequency. This approach is depicted in Figs. 10.14 and 10.15 for two subjects showing different patterns. Figures 10.14a and 10.14c show the percentage decrements of MDF and CV versus time for the TA of Subject 1 being stimulated at 20 Hz, 25 Hz, 30 Hz, 35 Hz, and 40 Hz.

In Figs. 10.14b and 10.14d the time scale has been replaced by the number of delivered pulses. The same presentation is provided in Fig. 10.15 for Subject 2 whose myoelectric manifestations of muscle fatigue are much greater than those of Subject 1. Although the curves of normalized MDF and CV versus the number of delivered pulses are much closer than those versus time, some difference exists, possibly due to the frequency effect on muscle vascularization, ischemia level, or other factors. The plots of Figs. 10.14 and 10.15 suggest that the differences between the two subjects might reflect differences in fiber constituency or vascularization of the respective muscles [89].

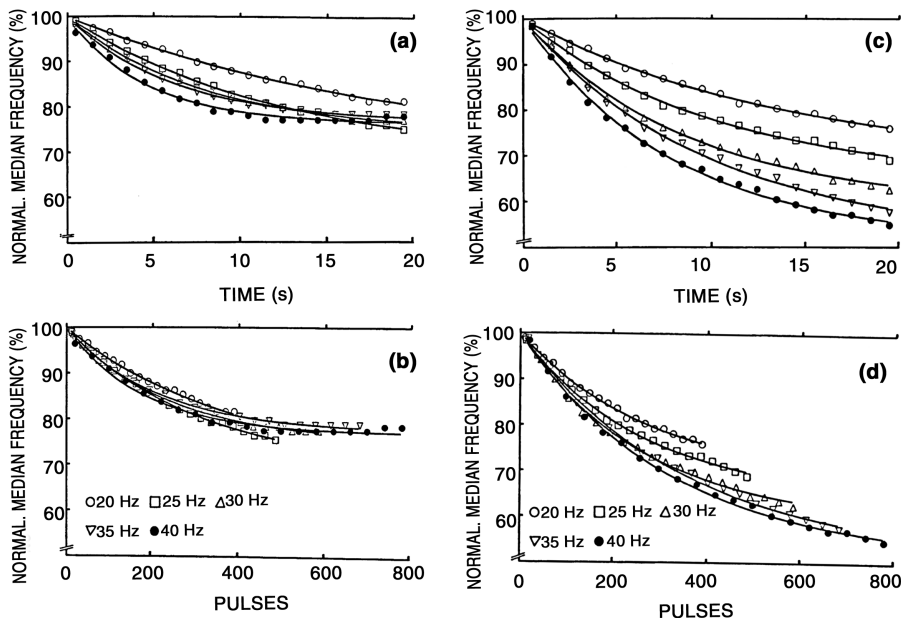


FIGURE 10.15 Same data reported in Fig. 10.14 but for a different subject showing greater myoelectric manifestations of muscle fatigue. Reproduced from [89] with permission.

A further issue under investigation is the use of pulses with different amplitude and duration attempting to activate different nerve fibers (and therefore different motor unit groups) having different intensity-time curves as proposed by Neyroud et al. [100].

10.7 EMG POWER SPECTRUM AND FIBER-TYPING; A CONTROVERSIAL ISSUE

Muscle are made of fibers which can be roughly classified, according to their histologic and metabolic properties, into three main types: slow oxidative fibers (SO or type I, slow twitch), fast oxidative glycolytic fibers (FOG or type IIa), and fast glycolytic fibers (FG or type IIb, fast twitch). These properties (together with others, such as fiber diameter) are reflected into sEMG features describing fatigue [60,76,77,111]. A classic result, obtained from in vitro neuromuscular preparations of three rat muscles with different fiber type distribution, is depicted in Fig. 10.16 which shows different decrease rates of median frequency (MDF) obtained from electrically elicited EMG signals detected with an electrode pair placed on the muscle in an in vitro preparation [72]. After the data collection the three muscles were fiber typed and showed different percentages of the three types of fibers (Fig. 10.16). The percentage of cross-sectional area occupied by different fiber types was clearly related to the rate of change of MDF. However, this association is not

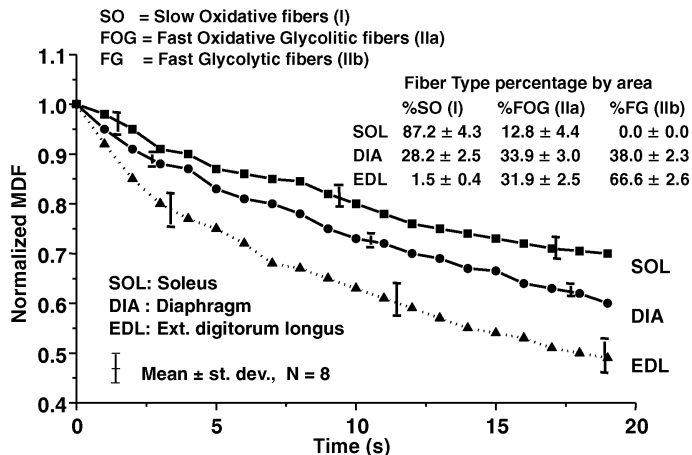


FIGURE 10.16 In vitro study of myoelectric manifestations of muscle fatigue. Normalized values of median frequency (MDF) were obtained from the soleus (SOL), diaphragm (DIA) and extensor digitorum longus (EDL) muscles of eight Wistar rats (mean \pm st. dev.). The neuro-muscular preparations were stimulated at 40 Hz for 20 s. Data for each muscle groups are normalized with respect to their initial values. The rate of change of MDF in the three muscles is correlated with the percentage of muscle cross section occupied by fast glycolytic fiber. Redrawn from [72] with permission.

straight-forward in vivo and in humans because of many other confounding factors, as discussed in Section 10.4 and in the following.

The conduction velocity with which an action potential propagates along a muscle fiber determines the duration of the generated waveform. Faster conduction velocity corresponds to shorter action potentials, and vice versa. Because the duration of an action potential is inversely associated with the bandwidth of its power spectrum, variables (or their changes) that are directly influenced by the spectral bandwidth of the sEMG signals have been traditionally associated to muscle fiber conduction velocity [74,75,80,123]. These considerations are at the basis of the observed myoelectric manifestations of muscle fatigue, as discussed in Chapter 4 and in this chapter. In addition to the association between *relative* decrease of conduction velocity and *relative* decrease of spectral variables (expressed as percentage change per second with respect to the initial value) commonly studied in the sEMG-based studies of fatigue, many researchers have tried to find an association between absolute values of spectral variables and the percentages of fibers of different type in a muscle. This association is based on the relations between conduction velocity and power spectrum and between fiber type and fiber size. The latter depends on the assumption that generally type I fibers have smaller diameter than type II fibers and therefore lower CV, resulting in lower MNF and MDF. Both associations, however, are only partially valid, as indicated in the following.

The association between fiber typing and fiber diameter is not direct. The distribution of conduction velocities of the fibers in a muscle is not bimodal but

presents a single peak [129] where it is not possible to distinguish different populations of fibers. Basically all other physiological properties of the muscle fibers follow a unimodal distribution [30,33]. Moreover, the association between type I fibers and small-diameter fibers is absent in back muscles [82,83].

The power spectrum of the sEMG is not influenced *only* by the muscle fiber conduction velocity. Other factors of influence are anatomical (e.g., subcutaneous layer thickness) and physiological (e.g., duration and shape of the intracellular action potentials) and are related to the recording method (e.g., type of derivation, electrode size, and interelectrode distance). These factors may vary between subjects and muscles and therefore make it questionable to compare absolute values of spectral variables for estimating the relative percentage of fiber typing [46,47,50]. Conversely, the relative changes of spectral variables over time with respect to their initial values are less influenced by the above mentioned factors, so that the rate of change of these variables have been used as a relatively robust index of fatigue [88].

For the above physiological and technical reasons, extracting indexes that characterize the percentage of fiber types in human muscles [83] or the proportion of fiber types used in a task [47,111,132,133] is a questionable approach.

10.8 REPEATABILITY OF MEASUREMENTS AND APPLICATIONS OF RESULTS

10.8.1 Repeatability of Measurements

Clinical applications of sEMG posit the reliability and repeatability testing of the techniques to be used for diagnosis and monitoring of patients. The repeatability of sEMG measurements and fatigue indicators has been tested by many researchers. Analysis of variance (ANOVA), coefficient of variation (CoV), standard error of the mean (SEM), and intraclass correlation coefficient (ICC) are widely used tools and indices. A critical issue concerning features of single-channel sEMG, obtained in different tests or days, is the repeatability of electrode position and interelectrode distance [44,73,96,108].

Rainoldi et al. [107] investigated the repeatability of amplitude (ARV), spectral parameters (MNF), and muscle fiber conduction velocity (CV) at four contraction levels in the biceps of 10 healthy subjects. Good inter- and intrasubject repeatability was found, in particular for CV values, although the rate of decrement (normalized with respect to the initial value) of MNF and CV showed differences among subjects, probably reflecting individual differences.

Fauth et al. [52] tested the reliability of RMS estimates of sEMG from the quadriceps and hamstring muscles, during isometric and ballistic activities, in 24 healthy subjects performing three repetitions. They found ICC mostly greater than 90%, intrasubjects CoV in the range of 11.5% to 49.3% and intersubject CoV in the range of 5.4% to 148%. They concluded that RMS is a reproducible quantity.

The long-term repeatability of RMS of shoulder and neck muscles was investigated by Røe et al. [113], who performed measurements over three years in 26 healthy subjects finding considerable intraindividual and interyear variations. Ollivier

et al. [102] compared the repeatability of estimates of RMS, MNF, and CV obtained from the biceps brachii of 10 healthy subjects using a bipolar pair of electrodes and a Laplacian (normal double differential) during isometric contractions at different levels. Not surprisingly the repeatability of the features obtained from one electrode pair was higher than that obtained with the Laplacian arrangement because of the higher spatial selectivity and smaller detection volume of the second method. Castroflorio et al. [10] tested the reproducibility of sEMG amplitude and spectral variables of jaw elevator muscles. Three voluntary contractions were performed at 80% MVC and the protocol was repeated in three days. ICC >70% was obtained only with an interelectrode distance of 30 mm—that is, with a very large detection volume. Zaman et al. [140] studied the decline of MNF of the biceps brachii during five weekly fatigue tests (sustained isometric contractions) performed on 11 participants and found the 95% confidence interval of the CoV to be 13.18% to 21.85%. Similar values were found for cyclic contractions.

Other reliability/repeatability studies were carried out on the quadriceps muscle [71,87], the back muscles [22,101,130], the biceps [107], the sternocleidomastoid, and anterior scalene muscles [34].

In general, the reproducibility of estimates of the sEMG features in isometric or dynamic conditions is not excellent; for this reason, its value in assessing the effectiveness of treatments or training procedures has been questioned. Only major changes can be detected. This observation is, in part, the result of the persisting lack of standards in the field. Despite the efforts of the European Project on “Surface Electromyography for Noninvasive Assessment of Muscles (SENIAM)” [63], most operators are not aware of the effects of changing electrode position and interelectrode distance on the estimates of sEMG features. Minor differences of this type in the repetition of an experimental protocol or task may have considerable impact on the results [21].

A substantial contribution to the issue of sEMG reliability and reproducibility may come, in the near future, from the use of electrode grids and from the automatic identification of regions of interest from which more reliable/repeatable signals can be extracted and fatigue indexes can be computed (Figs. 10.4, 10.8, and 10.9). It will also be possible to assess if the pool of the recruited motor units is the same or not in repeated contractions (see Chapter 7), thereby resolving one of the possible reasons of variability.

10.8.2 Applications of Results

Current findings on repeatability of results are still unsatisfactory, mostly due to the lack of standards and the inconsistent methodology. Nevertheless, sEMG has been used in a large number of clinical applications ranging from work-related disorders (see Chapter 13) to sport medicine, to studies of aging individuals, to “cancer fatigue,” and to a variety of pathologies (stroke, Parkinson disease, multiple sclerosis, diabetes). An excellent review concerning fatigue in central and peripheral nervous system disorders is provided in the work of Zwart et al. [143].

A few examples of clinical applications are summarized below. In 2006, Schulte et al. [117] observed, in eight individuals with painful trapezius muscle, an increased fatigue-related recruitment of motor units and a less pronounced decrement of CV,

with respect to healthy subjects. Falla et al. [34–36] investigated myoelectric manifestations of muscle fatigue in neck flexor muscles comparing the painful and nonpainful sides in patients with chronic unilateral neck pain. They revealed greater estimates of the initial value and slope of the MNF for both the sternocleidomastoid and anterior scalene muscles on the side of the patient's neck pain at 25% and 50% of MVC. Minetto et al. [97] conducted a single-blind, placebo-controlled study on the elbow flexors, knee extensors, and tibialis anterior of 20 men who received dexamethasone (8 mg/d) or placebo for one week. They observed an increase of voluntary muscle force and a smaller rate of decrease of MNF during voluntary contractions after treatment.

More recently, Minetto et al. [98] demonstrated that the levels of circulating muscle proteins, as well as CV and MNF of the sEMG, were significantly decreased in subjects affected by Cushing's disease. Differences between the CV values estimated in 10 patients and 30 controls were of the order of 23% to 26% for the knee extensors and 11.6% for the tibialis anterior. This association between biochemical and electrophysiological markers is of great interest for the follow up of myopathic patients and should be further investigated.

Watanabe et al. [134–136] investigated the knee extensors of nine type 2 diabetes mellitus patients at low-level voluntary contractions (10% MVC and 20% MVC) and found a smaller motor unit firing modulation and less spatial variability (lower entropy) of sEMG amplitude with respect to a healthy control group.

Rainoldi et al. [110] recorded sEMG signals from the vastus medialis longus (VML), the vastus medialis obliquus (VMO), and the vastus lateralis (VL) muscles during isometric knee extension contractions at 60% and 80% of the maximum voluntary contraction (MVC). They observed different myoelectric manifestations of fatigue that might be useful to noninvasively describe functional differences between the vasti muscles. The issue of load sharing, discussed in Section 10.2.2, may be relevant in this case, since the observed differences may be due to a different sharing of the load among these muscles in different subjects. This fact may be relevant in sport medicine.

It is reasonable to expect that a relation should exist between tissue oxygenation and myoelectric manifestations of muscle fatigue. Taelman et al. [125] found a strong correlation between MNF of the sEMG detected on the biceps brachii and the near-infrared spectroscopy results. Since both techniques provide information from the most superficial portion of a muscle, the combined information could be relevant with respect to such portion. Botter et al. [7] investigated the response of the vastus lateralis (VL) and vastus medialis longus (VML) to electrical stimulation finding that VL is more fatigable than VML and that motor units tend to be recruited, by increasing electrical stimulation intensity, in order of increasing CV in both muscles (see Chapter 11). Other authors investigated the effect of age and gender [86,129], cancer [69], and physical training [9] on myoelectric manifestations of muscle fatigue.

The agreement between sEMG-based estimation of fatigue and perceived exertion (assessed with the Borg scale), at least in isometric fatiguing contractions, is of considerable interest in occupational medicine [64,127].

In conclusion, while the modest reproducibility of sEMG features in repeated tests must be investigated and improved, the currently available techniques are applicable

in many situations where relatively large differences (greater than about 20%) are observed in sEMG features or in their rate of change with fatigue. The recent development of the sEMG imaging technology is very promising, in this regard, for the near future [55,70,136].

REFERENCES

1. Afsharipour, B., "Estimation of load sharing among muscles acting on the same joint and applications of surface electromyography," Ph.D. dissertation, Department of Electronics and Telecommunications, Politecnico di Torino, Torino, Italy, 2014.
2. Andreassen, S., and L. Arendt-Nielsen, "Muscle fibre conduction velocity in motor units of the human anterior tibial muscle: a new size principle parameter," *J. Physiol.* **391**, 561–571 (1987).
3. Arendt-Nielsen, L., and K. R. Mills, "The relationship between mean power frequency of the EMG spectrum and muscle fibre conduction velocity," *Electroencephalogr. Clin. Neurophysiol.* **60**, 130–134 (1985).
4. Bilodeau, M., A. B. Arsenault, D. Gravel, and D. Bourbonnais, "EMG power spectrum of elbow extensors: a reliability study," *Electromyogr. Clin. Neurophysiol.* **34**, 149–158 (1994).
5. Bonato, P., "From the guest editor - recent advancements in the analysis of dynamic EMG data," *Eng. Med. Biol. Mag. IEEE* **20**, 29–32 (2001).
6. Bonato, P., S. H. Roy, M. Knaflitz, and C. J. De Luca, "Time-frequency parameters of the surface myoelectric signal for assessing muscle fatigue during cyclic dynamic contractions," *IEEE Trans. Biomed. Eng.* **48**, 745–753 (2001).
7. Botter, A., F. Lanfranco, R. Merletti, and M. A. Minetto, "Myoelectric fatigue profiles of three knee extensor muscles," *Int. J. Sports Med.* **30**, 408–417 (2009).
8. Bouillard, K., A. Nordez, P. W. Hodges, C. Cornu, and F. Hug, "Evidence of changes in load sharing during isometric elbow flexion with ramped torque," *J. Biomechanics* **45**, 1424–1429 (2012).
9. Casale, R., A. Rainoldi, J. Nilsson, and P. Bellotti, "Can continuous physical training counteract aging effect on myoelectric fatigue? A surface electromyography study application," *Arch. Phys. Med. Rehabil.* **84**, 513–517 (2003).
10. Castroflorio, T., K. Icardi, B. Becchino, E. Merlo, C. Debernardi, P. Bracco, et al., "Reproducibility of surface EMG variables in isometric sub-maximal contractions of jaw elevator muscles," *J. Electromyogr. Kinesiol.* **16**, 498–505 (2006).
11. Chaffin, D. B., "Localized muscle fatigue—definiton and measurement," *J. Occupational Environ. Med.* **15**, 346–354 (1973).
12. Chowdhury, S. K., A. D. Nimbarde, M. Jaridi, and R. C. Creese, "Discrete wavelet transform analysis of surface electromyography for the fatigue assessment of neck and shoulder muscles," *J. Electromyogr. Kinesiol.* **23**, 995–1003 (2013).
13. Cifrek, M., V. Medved, S. Tonković, and S. Ostojić, "Surface EMG based muscle fatigue evaluation in biomechanics," *Clin. Biomech.* **24**, 327–340 (2009).
14. Contessa, P., and C. J. De Luca, "Neural control of muscle force: indications from a simulation model," *J. Neurophysiol.* **109**, 1548–1570 (2013).

15. Coorevits, P., L. Danneels, D. Cambier, H. Ramon, H. Druyts, J. S. Karlsson, et al., “Test–retest reliability of wavelet- and Fourier-based EMG (instantaneous) median frequencies in the evaluation of back and hip muscle fatigue during isometric back extensions,” *J. Electromyogr. Kinesiol.* **18**, 798–806 (2008).
16. Crenshaw, A., S. Karlsson, B. Gerdle, and J. Friden, “Differential responses in intramuscular pressure and EMG fatigue indicators during low versus high level isometric contractions to fatigue,” *Acta Physiol. Scand.* **160**, 353–361 (1997).
17. da Silva, R. A., C. Lariviere, A. B. Arsenault, S. Nadeau, and A. Plamondon, “The comparison of wavelet- and Fourier-based electromyographic indices of back muscle fatigue during dynamic contractions: validity and reliability results,” *Electromyogr. Clin. Neurophysiol.* **48**, 147–162 (2008).
18. De Luca, C. J., “Myoelectrical manifestations of localized muscular fatigue in humans,” *Crit. Rev. Biomed. Eng.* **11**, 251–279 (1984).
19. De Luca, C. J., “The use of surface electromyography in biomechanics,” *J. Appl. Biomech.* **13**, 135–163 (1997).
20. De Luca, C. J., and E. C. Hostage, “Relationship between firing rate and recruitment threshold of motoneurons in voluntary isometric contractions,” *J. Neurophysiol.* **104**, 1034–1046 (2010). Erratum in *J. Neurophysiol.* **107**(5):1544(2012).
21. De Nooij, R., L. A. C. Kallenberg, and H. J. Hermens, “Evaluating the effect of electrode location on surface EMG amplitude of the m. erector spinae p. longissimus dorsi,” *J. Electromyogr. Kinesiol.* **19**, e257–e266 (2009).
22. Dederling, Å., M. Roos af Hjelmsäter, B. Elfving, K. Harms-Ringdahl, and G. Németh, “Between-days reliability of subjective and objective assessments of back extensor muscle fatigue in subjects without lower-back pain,” *J. Electromyogr. Kinesiol.* **10**, 151–158 (2000).
23. Dideriksen, J. L., D. Farina, M. Baekgaard, and R. M. Enoka, “An integrative model of motor unit activity during sustained submaximal contractions,” *J. Appl. Physiol.* **108**, 1550–1562 (2010).
24. Dideriksen, J. L., D. Farina, and R. M. Enoka, “Influence of fatigue on the simulated relation between the amplitude of the surface electromyogram and muscle force,” *Philos. Trans. A Math. Phys. Eng. Sci.* **368**, 2765–2781 (2010).
25. Dideriksen, J. L., R. M. Enoka, and D. Farina, “Neuromuscular adjustments that constrain submaximal EMG amplitude at task failure of sustained isometric contractions,” *J. Appl. Physiol.* **111**, 485–494 (2011).
26. Dimitrov, G. V., T. I. Arabadzhiev, J. Y. Hogrel, and N. A. Dimitrova, “Simulation analysis of interference EMG during fatiguing voluntary contractions. Part II—changes in amplitude and spectral characteristics,” *J. Electromyogr. Kinesiol.* **18**, 35–43 (2008).
27. Dimitrov, G. V., Z. C. Lateva, and N. A. Dimitrova, “Effects of changes in asymmetry, duration and propagation velocity of the intracellular potential on the power spectrum of extracellular potentials produced by an excitable fiber,” *Electroencephalogr. Clin. Neurophysiol.* **28**, 93–100 (1988).
28. Dimitrova, N. A., and G. V. Dimitrov, “Interpretation of EMG changes with fatigue: facts, pitfalls, and fallacies,” *J. Electromyogr. Kinesiol.* **13**, 13–36 (2003).
29. Enoka, R. M., S. C. Gandevia, A. J. McComas, D. G. Stuart, C. K. E. Thomas, and P. A. Pierce, *Fatigue: Neural Control and Muscular Mechanisms*, vol. **384**, Plenum Press, New York, 1995.

30. Enoka, R. M., "Neural adaptations with chronic physical activity," *J. Biomech.* **30**, 447–455 (1997).
31. Enoka, R. M., and J. Duchateau, "Muscle fatigue: what, why and how it influences muscle function," *J. Physiol.* **586**, 11–23 (2008).
32. Enoka, R. M., S. Baudry, T. Rudroff, D. Farina, M. Klass, and J. Duchateau, "Unraveling the neurophysiology of muscle fatigue," *J. Electromyogr. Kinesiol.* **21**, 208–219 (2011).
33. Enoka, R. M., "Muscle fatigue—from motor units to clinical symptoms," *J. Biomech.* **45**, 427–433 (2012).
34. Falla, D., P. Dall'Alba, A. Rainoldi, R. Merletti, and G. Jull, "Repeatability of surface EMG variables in the sternocleidomastoid and anterior scalene muscles," *Eur. J. Appl. Physiol.* **87**, 542–549 (2002).
35. Falla, D., A. Rainoldi, R. Merletti, and G. Jull, "Myoelectric manifestations of sternocleidomastoid and anterior scalene muscle fatigue in chronic neck pain patients," *Clin. Neurophysiol.* **114**, 488–495 (2003).
36. Falla, D., G. Jull, A. Rainoldi, and R. Merletti, "Neck flexor muscle fatigue is side specific in patients with unilateral neck pain," *Eur. J. Pain* **8**, 71–77 (2004).
37. Farina, D., R. Merletti, A. Rainoldi, M. Buonocore, and R. Casale, "Two methods for the measurement of voluntary contraction torque in the biceps brachii muscle," *Med. Eng. Phys.* **21**, 533–540 (1999).
38. Farina, D., and R. Merletti, "Comparison of algorithms for estimation of EMG variables during voluntary isometric contractions," *J. Electromyogr. Kinesiol.* **10**, 337–349 (2000).
39. Farina, D., and R. Merletti, "Effect of electrode shape on spectral features of surface detected motor unit action potentials," *Acta Physiol. Pharmacol. Bulg.* **26**, 63–66 (2001).
40. Farina, D., R. Merletti, M. Nazzaro, and I. Caruso, "Effect of joint angle on EMG variables in leg and thigh muscles," *Eng. Med. Biol. Mag. IEEE* **20**, 62–71 (2001).
41. Farina, D., R. Merletti, B. Indino, M. Nazzaro, and M. Pozzo, "Surface EMG crosstalk between knee extensor muscles: experimental and model results," *Muscle & Nerve* **26**, 681–695 (2002).
42. Farina, D., L. Fattorini, F. Felici, and G. Filligoi, "Nonlinear surface EMG analysis to detect changes of motor unit conduction velocity and synchronization," *J. Appl. Physiol.* **93**, 1753–1763 (2002).
43. Farina, D., P. Madeleine, T. Graven-Nielsen, R. Merletti, and L. Arendt-Nielsen, "Standardising surface electromyogram recordings for assessment of activity and fatigue in the human upper trapezius muscle," *Eur. J. Appl. Physiol.* **86**, 469–478 (2002).
44. Farina, D., C. Cescon, and R. Merletti, "Influence of anatomical, physical, and detection-system parameters on surface EMG," *Biol. Cybern.* **86**, 445–456 (2002).
45. Farina, D., L. Mesin, S. Martina, and R. Merletti, "A surface EMG generation model with multilayer cylindrical description of the volume conductor," *IEEE Trans. Biomed. Eng.* **51**, 415–426 (2004).
46. Farina D., R Merletti, and R. Enoka, "The extraction of neural strategies from the surface EMG," *J. Appl. Physiol. (1985)* **96**, 1486–1495 (2004).
47. Farina, D., "Counterpoint: spectral properties of the surface EMG do not provide information about motor unit recruitment and muscle fiber type," *J. Appl. Physiol. (1985)* **105**, 1673–1674 (2008).

48. Farina, D., F. Leclerc, L. Arendt-Nielsen, O. Buttelli, and P. Madeleine, “The change in spatial distribution of upper trapezius muscle activity is correlated to contraction duration,” *J. Electromyogr. Kinesiol.* **18**, 16–25 (2008).
49. Farina, D., C. Cescon, F. Negro, and R. M. Enoka, “Amplitude cancellation of motor-unit action potentials in the surface electromyogram can be estimated with spike-triggered averaging,” *J. Neurophysiol.* **100**, 431–440 (2008).
50. Farina D., R. Merletti, and R. Enoka, “The extraction of neural strategies from the surface EMG: an update,” *J. Appl. Physiol. (1985)* **117**, 1215–1230 (2014).
51. Fattorini, L., F. Felici, G. C. Filligoi, M. Traballesi, and D. Farina, “Influence of high motor unit synchronization levels on non-linear and spectral variables of the surface EMG,” *J. Neurosci. Methods* **143**, 133–139 (2005).
52. Fauth, M. L., E. J. Petushek, C. R. Feldmann, B. E. Hsu, L. R. Garceau, B. N. Lutsch, et al., “Reliability of surface electromyography during maximal voluntary isometric contractions, jump landings, and cutting,” *J. Strength Cond. Res.* **24**, 1131–1137 (2010).
53. Filligoi, G., and F. Felici, “Detection of hidden rhythms in surface EMG signals with a non-linear time-series tool,” *Med. Eng. Phys.* **21**, 439–448 (1999).
54. Fuglevand, A. J., D. A. Winter, and A. E. Patla, “Models of recruitment and rate coding organization in motor-unit pools,” *J. Neurophysiol.* **70**, 2470–2488 (1993).
55. Gallina, A., R. Merletti, and T. M. M. Vieira, “Are the myoelectric manifestations of fatigue distributed regionally in the human medial gastrocnemius muscle?,” *J. Electromyogr. Kinesiol.* **21**, 929–938 (2011).
56. Gandevia, S., R. Enoka, A. McComas A., D. Stuart, and C. Thomas, *Fatigue: Neural and Muscular Mechanisms*, Plenum Press, New York, 1995.
57. Gandevia, S. C., “Spinal and supraspinal factors in human muscle fatigue,” *Physiol. Rev.* **81**, 1725–1789 (2001).
58. Gazzoni, M., F. Camelia, and D. Farina, “Conduction velocity of quiescent muscle fibers decreases during sustained contraction,” *J. Neurophysiol.* **94**, 387–394 (2005).
59. Gazzoni, M., D. Farina, and R. Merletti, “Motor unit recruitment during constant low force and long duration muscle contractions investigated with surface electromyography,” *Acta Physiol. Pharmacol. Bulg.* **26**, 67–71 (2001).
60. Gerdle, B., K. Henriksson-Larsén, R. Lorentzon, and M. L. Wretling, “Dependence of the mean power frequency of the electromyogram on muscle force and fibre type,” *Acta Physiol. Scand.* **142**, 457–465 (1991).
61. Gitter, J. A., and M. J. Czerniecki, “Fractal analysis of the electromyographic interference pattern,” *J. Neurosci. Methods* **58**, 103–108 (1995).
62. Herbert, R. D., and S. C. Gandevia, “Twitch interpolation in human muscles: Mechanisms and implications for measurement of voluntary activation,” *J. Neurophysiol.* **82**, 2271–2283 (1999).
63. Hermens, H., B. Freriks, R. Merletti, D. Stegeman, J. Blok, G. Rau, C. Disselhorst-Klug, G. Hägg, “European recommendations for surface electromyography: results of the SENIAM Project,” Roessing Research and Development, Enschede, The Netherlands, www.seniam.org, 1999.
64. Hummel, A., T. Läubli, M. Pozzo, P. Schenk, S. Spillmann, and A. Klipstein, “Relationship between perceived exertion and mean power frequency of the EMG signal from the upper trapezius muscle during isometric shoulder elevation,” *Eur. J. Appl. Physiol.* **95**, 321–326 (2005).

65. Inman, V. T., H. J. Ralston, J. B. De C. M. Saunders, M. B. Bertram Feinstein, and E. W. Wright Jr, "Relation of human electromyogram to muscular tension," *Electroencephalogr. Clin. Neurophysiol.* **4**, 187–194 (1952).
66. Islam, M. A., K. Sundaraj, R. B. Ahmad, and N. U. Ahamed, "Mechanomyogram for muscle function assessment: a review," *PLoS One* **8**, e58902 (2013).
67. Karlsson, S., Y. Jun, and M. Akay, "Enhancement of spectral analysis of myoelectric signals during static contractions using wavelet methods," *IEEE Trans. Biomed. Eng.* **46**, 670–684 (1999).
68. Karlsson, S., Y. Jun, and M. Akay, "Time-frequency analysis of myoelectric signals during dynamic contractions: a comparative study," *Trans. Biomed. Eng. IEEE* **47**, 228–238 (2000).
69. Kisiel-Sajewicz, K., V. Siemionow, D. Seyidova-Khoshknabi, M. P. Davis, A. Wyant, V. K. Ranganathan, et al., "Myoelectrical manifestation of fatigue less prominent in patients with cancer related fatigue," *PLoS One* **8**, e83636 (2013).
70. Kleine, B., N. Schumann, D. Stegeman, and H. Scholle, "Surface EMG mapping of the human trapezius muscle: the topography of monopolar and bipolar surface EMG amplitude and spectrum parameters at varied forces and in fatigue," *Clin. Neurophysiol.* **111**, 686–693 (2000).
71. Kollmitzer, J., G. R. Ebenbichler, and A. Kopf, "Reliability of surface electromyographic measurements," *Clin. Neurophysiol.* **110**, 725–734 (1999).
72. Kupa, E. J., S. H. Roy, S. C. Kandarian, and C. J. De Luca, "Effects of muscle fiber type and size on EMG median frequency and conduction velocity," *J. Appl. Physiol.* **79**, 23–32 (1995).
73. Li, W., and K. Sakamoto, "The influence of location of electrode on muscle fiber conduction velocity and EMG power spectrum during voluntary isometric contraction measured with surface array electrodes," *Appl. Hum. Sci.* **15**, 25–32 (1996).
74. Lindstrom, L., R. Magnusson, and I. Petersen, "Muscular fatigue and action potential conduction velocity changes studied with frequency analysis of EMG signals," *Electromyography* **10**, 341–356 (1970).
75. Lindstrom, L. H., and R. I. Magnusson, "Interpretation of myoelectric power spectra: a model and its applications," *Proc. IEEE* **65**, 653–662 (1977).
76. Linssen, W. H. J. P., M. Jacobs, D. F. Stegeman, E. M. G. Joosten, and J. Moleman, "Muscle fatigue in McArdle's disease: muscle fiber conduction velocity and surface EMG frequency spectrum during ischaemic exercise," *Brain* **113**, 1779–1793 (1990).
77. Linssen, W. H., D. F. Stegeman, E. M. Joosten, R. A. Binkhorst, M. J. Merks, H. J. ter Laak, et al., "Fatigue in type I fiber predominance: a muscle force and surface EMG study on the relative role of type I and type II muscle fibers," *Muscle Nerve* **14**, 829–837 (1991).
78. Lo Conte, L. R., and R. Merletti, "Advances in processing of surface myoelectric signals: Part 2," *Medical and Biological Engineering and Computing* **33**, 373–384 (1995).
79. Lo Conte, L. R., R. Merletti, and G. V. Sandri, "Hermite expansions of compact support waveforms: applications to myoelectric signals," *IEEE Trans. Biomed. Eng.* **41**, 1147–1159 (1994).
80. Lowery, M. M., C. L. Vaughan, P. J. Nolan, and M. J. O'Malley, "Spectral compression of the electromyographic signal due to decreasing muscle fiber conduction velocity," *IEEE Transactions on Rehabilitation Engineering* **8**, 353–361 (2000).
81. Maluf, K., M. Shinohara, J. Stephenson, and R. Enoka, "Muscle activation and time to task failure differ with load type and contraction intensity for a human hand muscle," *Exp. Brain Res.* **167**, 165–177 (2005).

82. Mannion, A. F., G. A. Dumas, R. G. Cooper, F. J. Espinosa, M. W. Faris, and J. M. Stevenson, "Muscle fibre size and type distribution in thoracic and lumbar regions of erector spinae in healthy subjects without low back pain: normal values and sex differences," *J. Anat.* **190**(Pt 4), 505–513 (1997).
83. Mannion, A. F., G. A. Dumas, J. M. Stevenson, and R. G. Cooper, "The influence of muscle fiber size and type distribution on electromyographic measures of back muscle fatigability," *Spine (Phila Pa 1976)* **23**, 576–584 (1998).
84. McKenzie, D. K., B. Bigland-Ritchie, R. B. Gorman, and S. C. Gandevia, "Central and peripheral fatigue of human diaphragm and limb muscles assessed by twitch interpolation," *J. Physiol.* **454**, 643–656 (1992).
85. Merletti, R., "Surface electromyography: possibilities and limitations," *J. Rehabil. Sciences* **7**, 25–34 (1994).
86. Merletti, R., D. Farina, M. Gazzoni, and M. P. Schieroni, "Effect of age on muscle functions investigated with surface electromyography," *Muscle & Nerve* **25**, 65–76 (2002).
87. Merletti, R., A. Fiorito, L. R. Lo Conte, and C. Cisari, "Repeatability of electrically evoked EMG signals in the human vastus medialis muscle," *Muscle & Nerve* **21**, 184–193 (1998).
88. Merletti, R., M. Knaflitz, and C. J. De Luca, "Myoelectric manifestations of fatigue in voluntary and electrically elicited contractions," *J. Appl. Physiol.* **69**, 1810–1820 (1990).
89. Merletti, R., M. Knaflitz, and C. J. De Luca, "Electrically evoked myoelectric signals," *Crit. Rev. Biomed. Eng.* **19**, 293–340 (1992).
90. Merletti, R., and L. R. Lo Conte, "Surface EMG signal processing during isometric contractions," *J. Electromyogr. Kinesiol.* **7**, 241–250 (1997).
91. Merletti, R., L. R. Lo Conte, and D. Sathyan, "Repeatability of electrically-evoked myoelectric signals in the human tibialis anterior muscle," *J. Electromyogr. Kinesiol.* **5**, 67–80 (1995).
92. Merletti, R., and P. A. Parker, eds., *Electromyography: Physiology, Engineering, and Noninvasive Applications*, IEEE Press and John Wiley & Sons, Hoboken, NJ, 2004.
93. Merletti, R., and S. Roy, "Myoelectric and mechanical manifestations of muscle fatigue in voluntary contractions," *J. Orthop. Sports Phys. Ther.* **24**, 342–353 (1996).
94. Mesin, L., C. Cescon, M. Gazzoni, R. Merletti, and A. Rainoldi, "A bi-dimensional index for the selective assessment of myoelectric manifestations of peripheral and central muscle fatigue," *J. Electromyogr. Kinesiol.* **19**, 851–863 (2009).
95. Mesin, L., M. Joubert, T. Hanekom, R. Merletti, and D. Farina, "A finite element model for describing the effect of muscle shortening on surface EMG," *IEEE Trans. Biomed. Eng.* **53**, 593–600 (2006).
96. Mesin, L., R. Merletti, and A. Rainoldi, "Surface EMG: the issue of electrode location," *J. Electromyogr. Kinesiol.* **19**, 719–726 (2009).
97. Minetto, M. A., A. Botter, F. Lanfranco, M. Baldi, E. Ghigo, and E. Arvat, "Muscle fiber conduction slowing and decreased levels of circulating muscle proteins after short-term dexamethasone administration in healthy subjects," *J. Clin. Endocrinol. Metab.* **95**, 1663–1671 (2010).
98. Minetto, M. A., F. Lanfranco, A. Botter, G. Motta, G. Mengozzi, R. Giordano, et al., "Do muscle fiber conduction slowing and decreased levels of circulating muscle proteins represent sensitive markers of steroid myopathy? A pilot study in Cushing's disease," *Eur. J. Endocrinol.* **164**, 985–993 (2011).

99. Molinari, F., M. Knaflitz, P. Bonato, and M. V. Actis, "Electrical manifestations of muscle fatigue during concentric and eccentric isokinetic knee flexion–extension movements," *IEEE Trans. Biomed. Eng.* **53**, 1309–1316 (2006).
100. Neyroud, D., D. Dodd, J. Gondin, N. A. Maffuletti, B. Kayser, and N. Place, "Wide-pulse-high-frequency neuromuscular stimulation of triceps surae induces greater muscle fatigue compared with conventional stimulation," *J. Appl. Physiol.* **116**, 1281–1289 (2014).
101. Ng, J. K. F., and C. A. Richardson, "Reliability of electromyographic power spectral analysis of back muscle endurance in healthy subjects," *Arch. Phys. Med. Rehabil.* **77**, 259–264 (1996).
102. Ollivier, K., P. Portero, O. Maïsetti, and J.-Y. Hogrel, "Repeatability of surface EMG parameters at various isometric contraction levels and during fatigue using bipolar and Laplacian electrode configurations," *J. Electromyogr. Kinesiol.* **15**, 466–473 (2005).
103. Pedrinelli, R., L. Marino, G. Dell'Osso, G. Siciliano, and B. Rossi, "Altered surface myoelectric signals in peripheral vascular disease: correlations with muscle fiber composition," *Muscle & Nerve* **21**, 201–210 (1998).
104. Piper, H. E., *Electrophysiologie, Menschlicher Muskeln*, J. Springer, Berlin, 1912.
105. Poli, R., J. Kennedy, and T. Blackwell, "Particle swarm optimization," *Swarm Intell.* **1**, 33–57 (2007).
106. Pozzo, M., E. Merlo, D. Farina, G. Antonutto, R. Merletti, and P. Di Prampero, "Muscle fiber conduction velocity estimated from surface EMG signals during explosive dynamic contractions," *Muscle & Nerve* **29**, 823–833 (2004).
107. Rainoldi, A., G. Galardi, L. Maderna, G. Comi, L. Lo Conte, and R. Merletti, "Repeatability of surface EMG variables during voluntary isometric contractions of the biceps brachii muscle," *J. Electromyogr. Kinesiol.* **9**, 105–119 (1999).
108. Rainoldi, A., M. Nazzaro, R. Merletti, D. Farina, I. Caruso, and S. Gaudenti, "Geometrical factors in surface EMG of the vastus medialis and lateralis muscles," *J. Electromyogr. Kinesiol.* **10**, 327–336 (2000).
109. Rainoldi, A., J. E. Bullock-Saxton, F. Cavarretta, and N. Hogan, "Repeatability of maximal voluntary force and of surface EMG variables during voluntary isometric contraction of quadriceps muscles in healthy subjects," *J. Electromyogr. Kinesiol.* **11**, 425–438 (2001).
110. Rainoldi, A., D. Falla, R. Mellor, K. Bennell, and P. Hodges, "Myoelectric manifestations of fatigue in vastus lateralis, medialis obliquus and medialis longus muscles," *J. Electromyogr. Kinesiol.* **18**, 1032–1037 (2008).
111. Rainoldi, A., M. Gazzoni, and G. Melchiorri, "Differences in myoelectric manifestations of fatigue in sprinters and long distance runners," *Physiol. Meas.* **29**, 331–340 (2008).
112. Rix, H., and J. P. Malengé, "Detecting small variations in shape," *IEEE Trans. Syst. Man Cybern.* **10**, 90–96 (1980).
113. Røe, C., Ó. A. Steingrimsdóttir, S. Knardahl, E. S. Bakke, and N. K. Vøllestad, "Long-term repeatability of force, endurance time and muscle activity during isometric contractions," *J. Electromyogr. Kinesiol.* **16**, 103–113 (2006).
114. Rojas-Martínez, M., M. A. Mañas, J. F. Alonso, and R. Merletti, "Identification of isometric contractions based on high density EMG maps," *J. Electromyogr. Kinesiol.* **23**, 33–42 (2013).
115. Roy, S. H., C. J. De Luca, and J. Schneider, "Effects of electrode location on myoelectric conduction velocity and median frequency estimates," *J. Appl. Physiol.* **61**, 1510–1517 (1986).

116. Sadoyama, T., T. Masuda, H. Miyata, and S. Katsuta, “Fibre conduction velocity and fibre composition in human vastus lateralis,” *Eur. J. Appl. Physiol. Occup. Physiol.* **57**, 767–771 (1988).
117. Schulte, E., O. Miltner, E. Junker, G. Rau, and C. Disselhorst-Klug, “Upper trapezius muscle conduction velocity during fatigue in subjects with and without work-related muscular disorders: a non-invasive high spatial resolution approach,” *Eur. J. Appl. Physiol.* **96**, 194–202 (2006).
118. Shield, A., and S. Zhou, “Assessing voluntary muscle activation with the twitch interpolation technique,” *Sports Med.* **34**, 253–267 (2004).
119. Singh, V. P., D. K. Kumar, B. Polus, and S. Fraser, “Strategies to identify changes in SEMG due to muscle fatigue during cycling,” *J. Med. Eng. Technol.* **31**, 144–151 (2007).
120. Sjøgaard, G., G. Savard, and C. Juel, “Muscle blood flow during isometric activity and its relation to muscle fatigue,” *Eur. J. Appl. Physiol.* **57**, 327–335 (1988).
121. Staudenmann, D., A. Daffertshofer, I. Kingma, D. F. Stegeman, and J. H. van Dieen, “Independent component analysis of high-density electromyography in muscle force estimation,” *IEEE Trans. Biomed. Eng.* **54**, 751–754 (2007).
122. Staudenmann, D., J. H. van Dieen, D. F. Stegeman, and R. M. Enoka, “Increase in heterogeneity of biceps brachii activation during isometric submaximal fatiguing contractions: a multichannel surface EMG study,” *J. Neurophysiol.* **111**, 984–890 (2014).
123. Stulen, F. B., and C. J. De Luca, “The relation between the myoelectric signal and physiological properties of constant-force isometric contractions,” *Electroencephalogr. Clin. Neurophysiol.* **45**, 681–698 (1978).
124. Stulen, F. B., and C. J. De Luca, “Frequency parameters of the myoelectric signal as a measure of muscle conduction velocity,” *IEEE Trans. Biomed. Eng.* **28**, 515–523 (1981).
125. Taelman, J., J. Vanderhaegen, M. Robijns, G. Naulaers, A. Spaepen, and S. Van Huffel, “Estimation of muscle fatigue using surface electromyography and near-infrared spectroscopy,” in *Oxygen Transport to Tissue XXXII*, vol. **701**, J. C. LaManna, M. A. Puchowicz, K. Xu, D. K. Harrison, and D. F. Bruley, eds., Springer, New York, pp. 353–359, 2011.
126. Tarata, M. T., “Mechanomyography versus electromyography, in monitoring the muscular fatigue,” *Biomed. Eng. Online* **2**, 3 (2003).
127. Troiano, A., F. Naddeo, E. Sosso, G. Camarota, R. Merletti, and L. Mesin, “Assessment of force and fatigue in isometric contractions of the upper trapezius muscle by surface EMG signal and perceived exertion scale,” *Gait & Posture* **28**, 179–186 (2008).
128. Troni, W., R. Cantello, and I. Rainero, “Conduction velocity along human muscle fibers in situ,” *Neurology* **33**, 1453–1459 (1983).
129. Tsuboi, H., Y. Nishimura, T. Sakata, H. Ohko, H. Tanina, K. Kouda, et al., “Age-related sex differences in erector spinae muscle endurance using surface electromyographic power spectral analysis in healthy humans,” *Spine J.* **13**, 1928–1933 (2013).
130. van Dieen, J. H., and P. Heijblom, “Reproducibility of isometric trunk extension torque, trunk extensor endurance, and related electromyographic parameters in the context of their clinical applicability,” *J. Orthop. Res.* **14**, 139–143 (1996).
131. Viitasalo, J. H. T., and P. V. Komi, “Signal characteristics of EMG with special reference to reproducibility of measurements,” *Acta Physiol. Scand.* **93**, 531–539 (1975).
132. von Tscharner, V., and B. M. Nigg, “Point: spectral properties of the surface EMG can characterize/do not provide information about motor unit recruitment strategies and muscle fiber type,” *J. Appl. Physiol.* (1985) **105**, 1671–1674 (2008).

133. Wakeling, J. M., S. A. Pascual, and B. M. Nigg, "Altering muscle activity in the lower extremities by running with different shoes," *Med. Sci. Sports Exerc.* **34**, 1529–1532 (2002).
134. Watanabe K., T. Miyamoto, Y. Tanaka, K. Fukuda, and T. Moritani, "Type 2 diabetes mellitus patients manifest characteristic spatial EMG potential distribution pattern during sustained isometric contraction," *Diabetes Res. Clin. Pract.* **97**, 468–473 (2012).
135. Watanabe, K., M. Gazzoni, A. Holobar, T. Miyamoto, K. Fukuda, R. Merletti, and T. Moritani, "Motor unit firing pattern of vastus lateralis muscle in type 2 diabetes mellitus patients," *Muscle & Nerve* **48**, 806–813 (2013).
136. Watanabe, K., M. Kouzaki, and T. Moritani, "Region-specific myoelectric manifestations of fatigue in human rectus femoris muscle," *Muscle & Nerve* **48**, 226–234 (2013).
137. Westgaard, R. H., and C. J. De Luca, "Motor unit substitution in long-duration contractions of the human trapezius muscle," *J. Neurophysiol.* **82**, 501–504 (1999).
138. Yao, W., R. J. Fuglevand, and R. M. Enoka, "Motor-unit synchronization increases EMG amplitude and decreases force steadiness of simulated contractions," *J. Neurophysiol.* **83**, 441–452 (2000).
139. Yassierli, and M. A. Nussbaum, "Utility of traditional and alternative EMG-based measures of fatigue during low-moderate level isometric efforts," *J. Electromyogr. Kinesiol.* **18**, 44–53 (2008).
140. Zaman, S. A., D. T. MacIsaac, and P. A. Parker, "Repeatability of surface EMG-based single parameter muscle fatigue assessment strategies in static and cyclic contractions," in *Engineering in Medicine and Biology Society, EMBC, 2011 Annual International Conference of the IEEE*, pp. 3857–3860, 2011.
141. Zijdewind, I., and D. Kernell, "Fatigue associated EMG behavior of the first dorsal interosseous and adductor pollicis muscles in different groups of subjects," *Muscle & Nerve* **17**, 1044–1054 (1994).
142. Zijdewind, I., M. J. Zwarts, and D. Kernell, "Fatigue-associated changes in the electromyogram of the human first dorsal interosseous muscle," *Muscle & Nerve* **22**, 1432–1436 (1999).
143. Zwart M., G. Bleijenberg, and B. van Engelen, "Clinical neurophysiology of fatigue," *Clin. Neurophysiol.* **119**, 2–10 (2008).